UDC544.31:546.56'22/24

THERMODYNAMIC PROPERTIES OF COMPLEX COPPER CHALCOGENIDES REVIEW

[1,2,3]M.B. Babanly*, [1]L.F. Mashadiyeva, [1]S.Z. Imamaliyeva, [1]D.B. Tagiev, [1,4]D.M. Babanly, [5]Yu.A. Yusibov

[1]Institute of Catalysis and Inorganic Chemistry named after. M. Nagieva MSE AR
[2]Baku State University
[3]Azerbaijan State University of Economics
[4]French - Azerbaijani University (UFAZ), Azerbaijan, Baku
[5]Ganja State University
**e-mail: babanlymb@gmail.com*

Received 21.03.2024
Accepted 13.05.2024

Abstract: *Complex copper-based chalcogenides are a significant environmental-friendly functional material that has great application potential due to their interesting thermoelectric, photoelectric, optical, and other properties, as well as their ionic conductivity. Analysis of numerous studies shows that improving the application characteristics of these compounds is associated with manipulating their structure and composition. An effective solution for optimizing such processes requires their in-depth thermodynamic analysis, which requires reliable data on the fundamental thermodynamic characteristics of the corresponding compounds. This review summarizes the results of researches, including ours works, on the thermodynamic properties of copper chalcogenides with some p^1-p^3 elements. The majority of these works were carried out using various modifications of the electromotive force (EMF) method. Planning of experiments carried out by this equilibrium method of chemical thermodynamics and processing of their data is impossible without the presence of reliable data on phase equilibria. Taking this into account, in addition to thermodynamic data, the work also presents the solid-phase equilibria diagrams for a number of systems studied by the EMF method.*

The analysis showed that for the Cu-Tl-X, Cu-Ge(Sn)-X (X-S, Se, Te) and Cu-As(Sb, Bi)-S(Se) ternary systems there are mutually consistent data on the phase equilibria and thermodynamic functions of the ternary compounds. For the Cu-Tl-X and Cu-Sn-Se systems, the thermodynamic functions of ternary compounds are obtained by two modifications of the EMF method by determining the partial molar functions of two different components - copper and thallium (tin). The thermodynamic properties of copper chalcogenides with gallium, indium, and silicon have not been extensively researched, and the data that is available is inconsistent.

Keywords*: complex copper chalcogenides, ternary copper-containing systems, phase diagrams, thermodynamic properties, EMF method.*
DOI: 10.32737/2221-8688-2024-3-243-280

1. Introduction

Binary and complex metal chalcogenides have been widely studied since the middle of the last century as semiconductor, thermoelectric, photoelectric, optical, magnetic, and other functional materials. Many of them have found applications or are considered promising for use in various fields of modern engineering and technology [1-7]. The development of nanomaterials science and the discovery of new unique quantum states of matter as a topological insulator [8], and then an antiferromagnetic topological insulator [9], gave new impetus to the research of chalcogenides. Studies have shown that many-layered chalcogenides have the properties of a topological insulator [10-14], and some of them

combine the properties of a topological insulator and a magnet [15-17] and are extremely promising for a wide variety of applications in modern high technologies [18-20].

Copper-based chalcogenides occupy an important place among advanced functional materials. In addition to unique electronic properties [3-5, 21-29], they also have high ionic conductivity [30-33] and are considered very promising for use in thermoelectric and photoelectric energy converters and optoelectronic devices, as well as solid-state electrodes and electrolytes, selective membranes, sensors, sensors, etc. Moreover, according to a number of studies in recent years, some copper-based chalcogenides are promising for use in medicine [34, 35]. On the other hand, many copper chalcogenides exist in nature in the form of minerals and are of great interest to the geochemistry of the earth [36, 37].

Analysis of numerous studies on complex copper-containing chalcogenide materials (see Sections 3-5) shows the possibility of significantly improving their functional properties by manipulating the structure and composition. For a better understanding of the relationship between composition, structure and properties, as well as for the search and design of new materials, it is especially important to have reliable, mutually consistent data on the phase equilibria and thermodynamic properties of the corresponding systems [20, 38-40]. The importance of using phase diagrams is that they make it possible not only to identify new compounds or phases of variable composition but also to establish their thermal stability, the nature of formation, areas of primary crystallization and homogeneity, the presence of phase transformations, etc. An effective solution to the optimization of processes requires a deeper thermodynamic analysis, which is only possible if reliable data are available on the fundamental thermodynamic characteristics of the relevant compounds [38].

The purpose of this review is to systematize existing literature data, including the authors' work on the study of the thermodynamic properties of copper chalcogenides with heavy p^1-p^3 elements.

Section 2 of the manuscript briefly describes some methodological issues related to thermodynamic research, especially the electromotive force (EMF) method, which was employed to obtain most thermodynamic data for copper-based chalcogenides. In the following sections, available data on the fundamental thermodynamic characteristics of these ternary compounds and some phases based on them are presented and discussed. Considering the importance of phase diagrams in EMF studies, this manuscript also presents data on solid-phase equilibria of a number of studied systems in addition to thermodynamic dat. At the beginning of these sections, a brief overview of works on the most characteristic functional properties of ternary phases of this type is given. The EMF method is employed to obtain thermodynamic data for copper-based chalcogenides.

2. Some methodological issues in the thermodynamic study of metal chalcogenides

An analysis of numerous literature data shows that the EMF method occupies a leading position in the thermodynamic study of metallic and semiconductor, in particular chalcogenide, systems. Various modifications of this method, such as the classical version of concentration cells with a liquid electrolyte, the EMF method with a solid cation- and anion-conducting electrolyte, accelerated modifications of the method, etc. are successfully used in thermodynamic research [41-45].

An important advantage of the EMF method is that it is an equilibrium method of chemical thermodynamics and allows combining thermodynamic research with phase equilibria studies [42, 43]. At the same time, phase equilibria data is important for both experiment planning using the EMF method and processing results.

In practice, thermodynamic studies most often use concentration cells relative to electrodes of the following type [41-43]

(–) A (solid or liquid) | ionic conductor containing ions A^{z+} | A in alloys (+) (1)

where A is the least noble component of the studied system.

EMF measurement data in a certain temperature range are presented in the form of linear equations, for example, in the form

$$E = a + bT \pm t\left[\frac{S_E^2}{n} + S_b^2(T-\overline{T})^2\right]^{1/2} \quad (2)$$

recommended in [42]. Here *n* - is the number of pairs of values *E* and *T*; S_E and S_b are the dispersions of individual EMF measurements and coefficient *b*, respectively; $\overline{T}$ - the average absolute temperature; *t* – is Student's criterion. The Student's criterion is $t \leq 2$ with a confidence level of 95% and the number of experimental points being $n \geq 20$.

From equations (2) according to the following thermodynamic relations

$$\Delta\overline{G}_A = -zFE \quad (3)$$

$$\Delta\overline{S}_A = zF\left(\frac{\partial E}{\partial T}\right)_p \quad (4)$$

$$\Delta\overline{H}_A = -zF\left[E - T\left(\frac{\partial E}{\partial T}\right)_p\right] \quad (5)$$

the partial molar functions of the mobile component A may be calculated.

Thus, by measuring the equilibrium values of the EMF of concentration cells of type (1) in a wide temperature range for various compositions of the right-hand electrodes, it is possible to calculate the relative partial molar free energy, enthalpy and entropy of component A in a multicomponent solution or heterogeneous mixture.

The issues of organizing and conducting experiments using various variants of the EMF method and methods of mathematical processing of results are discussed in detail in a number of monographs and original works [42-49].

Due to the high accuracy of electrochemical measurements, the determination of thermodynamic functions by the EMF method gives reliable results. The root mean square error of EMF measurements under favorable conditions can be reduced to 0.5 mV, which corresponds to a single determination error of the order of 100 $J \cdot mol^{-1}$. This value decreases by another factor of $n^{1/2}$ (n is the number of experimental points) for the average value. Such accuracy is incomprehensible in other methods of thermodynamic study of condensed systems. Relative partial molar entropy and enthalpy, calculated from the temperature coefficient of EMF, are determined with less accuracy. However, experience shows that by ensuring the reversibility of the operation of electrochemical circuits in a wide temperature range, the accuracy of determination of and can reach $0.5 \div 1$ $J \cdot K^{-1} \cdot mol^{-1}$ and $0.3 \div 0.5$ $kJ \cdot mol^{-1}$, which is comparable with the accuracy of calorimetric measurements [42].

In [42-44], methods for calculating integral thermodynamic functions of ternary and more complex phases based on partial thermodynamic functions of potential-forming components and a phase diagram are described in detail.

Let's consider the main types of concentration cells used in thermodynamic studies of complex chalcogenides.

1) In several researches, including studies our group [43, 44, 50-55], concentration cells of the following type

$$\begin{matrix}(-)\ A\ (solid)\ \mid glycerol{+}A^{z+} \mid (A\ in\ alloy)\ (solid) \\ (+)\end{matrix} \quad (6)$$

were used in the thermodynamic study of chalcogenide systems.

Using of glycerol solutions of alkali or alkaline earth metals' chlorides makes it possible to conduct experiments in the 300-430 K temperature range, i.e. under conditions close to standard. It should be noted that electrochemical cells with glycerol electrolyte, first applied in 1963 by authors of [56] to amalgam systems, and later successfully used to study various binary and complex systems

2) The discovery of superionic conductors with pure Cu^+ and Ag^+ conductivity at room temperature, primarily the Ag_4RbI_5 [57] and $Cu_4RbI_3Cl_2$ compounds [58], gave new impetus to thermodynamic studies of copper- and silver-containing systems. In a number of works [59-63], concentration cells relative to a copper (silver) electrode with the indicated electrolytes were used to study ternary chalcogenides of copper and silver

(-) A^I (solid) |solid electolyte $+A^+$ | (A^I in alloys) (solid) (+) (7)

(here A^I is Cu^+ or Ag^+).

The authors of [64-67] successfully used concentration cells with glassy Ag^+ conducting electrolyte for thermodynamic studies of silver-containing systems.

It should be noted that to determine the thermodynamic functions of the formation of complex chalcogenide phases, including copper and silver, calorimetric methods are used relatively less frequently. This is apparently due to the complexity of calorimetric experiments, as well as the fact that during the synthesis or combustion of substances in a calorimetric bomb, the processes often do not proceed to completion and it is very difficult to quantify the degree of conversion [38, 43]

At the same time, the differential scanning calorimetry (DSC) is successfully used to determine the thermodynamic functions of reversible phase transitions of the first order - polymorphic transformations or melting [68-70].

3. Copper chalcogenides with elements of the gallium subgroup

Copper chalcogenides with gallium and indium, as well as solid solutions and doped phases based on them, are excellent materials for use in photovoltaic devices [71-84], optoelectronics [75, 85-87], and also as luminescent materials [88- 91].

The use of these phases as solar energy absorbers is due to their band gap, which correlates well with the maximum photon power density in the spectrum of sunlight and at the same time demonstrates long-term stability and resistance to radiation [82-84]. In the past few years, substantial research has been conducted to enhance their effectiveness. For this purpose, several studies have proposed changing the bulk or surface composition through sulfidization (selenidization) [77, 79, 80], adjusting the ratios of Cu, Ga, and In atoms [73, 84], adding alloying components [71, 78] and other strategies [78]. Note, that by sulfidization of the Cu(Ga, In)Se_2 layers, a solar cell with a record efficiency of 23.35% was obtained [81]. Thin-film solar cells based on Cu(Ga, In)Se_2 are considered as a promising for electricity generation in space stations [82, 84].

Authors of the review [76] using a fundamental thermodynamic approach discussed the main reasons for the relatively low efficiency of photovoltaic systems based on copper-gallium (indium) chalcogenides and ways to optimize methods for obtaining their crystals with specified characteristics. The latest advancements in the production of nanocrystals of these phases with controlled compositions and band gaps are presented in another review [78].

Copper chalcogenide compounds, which have a wide bandgap energy range, are very attractive for applications in optoelectronic and light-emitting devices [86]. Due to their unique optical properties, they can also be used in nonlinear optical devices [87]. The authors of [88] report the development of quantum dot LEDs that exhibit red color with a narrow emission peak by controlling the copper content of Cu-Ga-In-S alloys.

Copper selenides and tellurides with elements of the gallium subgroup, especially thallium, are of interest as thermoelectric materials with low thermal conductivity [92-95].

3.1. The Cu-Ga-X и Cu-In-X (X-S, Se, Te) systems

Copper with gallium and indium forms ternary phases with a wide homogeneity region, which have a disordered cubic structure. With decreasing temperature, these phases transform into low-temperature compounds with ordered structures. The most typical compounds are the $CuB^{III}X_2$, $CuB^{III}{}_3X_5$ and $CuB^{III}{}_5X_8$. These compounds form on Cu_2X-$B^{III}{}_2X_3$ quasi-binary sections and form stable connodes with the

corresponding elemental chalcogen [96-99].

We have not found any literature data on the thermodynamic properties of copper-gallium chalcogenides. The thermodynamic properties of copper-indium sulfides and selenides have been studied in a number of works (Table 1).

Table 1. Standard integral thermodynamic functions of ternary compounds of the Cu-Ga(In)-X systems

Compound	$-\Delta_f G^0(298K)$	$-\Delta_f H^0(298K)$	$S^0(298K)$	Ref.
	кJ·mol^{-1}		J·mol^{-1}·K^{-1}	
$CuIn_5S_8$	1238±113			[99]
$CuInS_2$	315±54	-		[99]
		221.8±13		[100]
		327.6	136±0.8 [30]	[101]
$CuIn_5Se_8$	1060			[102]
$CuIn_3Se_5$	380.0±1,4	398.2±28,6	373±28	[59]
	*467.1±28.0	*486.3±27.0		[59]
	658			[102]
$CuInSe_2$	153.2±0,6	158.0±9.6	163±11	[59]
	*196.8±9.8	*201.6±9.2		
	220.0	218.5		[102]

Note: * - values calculated from data [59] using other thermodynamic data for In_2Te_3.

Table 1 shows that the available data are insufficient and contradictory. Complete complexes of standard integral thermodynamic functions were determined only for compounds $CuIn_3Se_5$ and $CuInSe_2$ by the EMF method with a Cu+ conducting electrolyte (cell of type 7) [59]. For processing the experimental results, the authors of [54] used the following data for the In_2Se_3 compound: $-\Delta_f G^0(298K)$ = 224.3 ± 0.8 kJ/mol; $-\Delta_f H^0(298K)$=239.3 ± 18.4 kJ/mol; S^0_{298}=201.3 ± 16.7 J/(mol·K). Considering that modern reference books, for example [112], recommend significantly different from the above data ($\Delta_f H^0(298K)$ = -326.4±16.7 kJ/mol ; S^0_{298} = 201.3±16.7 J/(mol·K)), the latter was used in our calculations for $CuIn_3Se_5$ and $CuInSe_2$ (marked with an asterisk in Table 1). The data obtained for CuInSe2 are in better agreement with the results of [102].

3.2. The Cu-Tl-X systems

The results of multiple studies on phase equilibria and thermodynamic properties of these systems, carried out before the early 90s of the last century, are summarized in [21].

Below the results of thermodynamic studies, including more recent studies, as well as brief information of solid-phase equilibria in the appropriate system are given.

The Cu-Tl-S system. The Cu_2S-Tl_2S quasi-binary section of this system was studied almost simultaneously by two teams of authors [103, 104]. According to [103], this system is characterized by the formation of the Cu_9TlS_5, Cu_3TlS_2 and CuTlS ternary compounds. The first two compounds melt with decomposition by peritectic reactions at 706 and 693 K, respectively, and the last one melts congruently at 689 K. According to [104], there are two congruently melting ternary compounds CuTlS and $Cu_8Tl_2S_5$ in the system. The phase diagram presented in [103] was confirmed by the authors of [105].

The results of a comprehensive study of the phase equilibria of the Cu-Tl-S system are presented in [106-108]. The projection of the liquidus surface, solid-phase equilibria diagram at 300 K and a number of polythermal sections of the phase diagram are constructed. In [108], the results of a thermodynamic study of copper-thallium sulfides by EMF measurements of concentration cells of type (6) are also presented. Later, in [109], a thermodynamic study of the Cu-Tl-S system was carried out by

EMF measurements of concentration cells of type (7) relative to a copper electrode. It should be noted that the thermodynamic data obtained in [108, 109] are independent: they use the results of EMF measurements of different concentration cells, based on which the partial thermodynamic functions of various components of the system - thallium and copper are calculated, which characterize various potential-forming reactions.

Let us consider the results of these works in more detail. In **Fig.1** a solid-phase equilibria diagram of the Cu-Tl-S system is presented. This diagram is characterized by the presence of four ternary compounds, which form a series of three-phase regions between themselves, as well as with binary compounds and the initial components of the system. Tables 2 and 3 list the equations of type (2) for the temperature dependences of the EMF of cells of types (6) and (7).

Table 2. Temperature dependences of the EMF of concentration cells of type (6) in some phase areas of the Cu-Tl-S system (T=300÷380K) [108]

Phase area in Fig.1	$E, mV = a + bT \pm 2S_E(T)$
Cu_9TlS_5+Cu_2S+CuS	$580.0-0.044T \pm 2\left[\frac{2.4}{40}+0.0001(T-346.7)^2\right]^{1/2}$
Cu_3TlS_2+Cu_9TlS_5+CuS	$585.5+0.315T \pm 2\left[\frac{152}{40}+0.0035(T-349.6)^2\right]^{1/2}$
CuTlS+ Cu_3TlS_2+ $CuTlS_2$	$598.6+0.351T \pm 2\left[\frac{135}{88}+0.0017(T-351.5)^2\right]^{1/2}$
$CuTlS_2$+ CuS+S	$435.1+0.140T \pm 2\left[\frac{40}{57}+0.0006(T-350.6)^2\right]^{1/2}$

Table 3. Temperature dependences of the EMF of concentration cells of type (7) in some phase areas of the Cu-Tl-S system (T=300÷380K) [109]

Phase area in Fig.1	$E, mV = a + bT \pm 2S_E(T)$
$CuTlS_2$+TlS_2+S	$452.2-0.056T \pm 2\left[\frac{2.5}{24}+7.2\cdot10^{-5}(T-343.7)^2\right]^{1/2}$
CuTlS+$CuTlS_2$+Tl_4S_3	$389.4+0.086T \pm 2\left[\frac{2.7}{22}+9.7\cdot10^{-5}(T-346.1)^2\right]^{1/2}$
Cu_3TlS_2+$CuTlS_2$+ CuS	$340.2+0.067T \pm 2\left[\frac{1.8}{22}+5.8\cdot10^{-5}(T-344.1)^2\right]^{1/2}$
Cu_9TlS_5+Cu_3TlS_2+ CuS	$292.1+0.134T \pm 2\left[\frac{1.6}{22}+5.2\cdot10^{-5}(T-342.6)^2\right]^{1/2}$

From these equations, using relations (3)-(5), the relative partial thermodynamic functions of thallium (Table 4) and copper (Table 5) were calculated.

Table 4. Relative partial thermodynamic functions of thallium in Cu-Tl-S alloys at 298 K

Phase area in Fig.1	$-\Delta\overline{G}_{Tl}$	$-\Delta\overline{H}_{Tl}$	$\Delta\overline{S}_{Tl}$
	кJ·mol^{-1}		J·mol^{-1} K^{-1}
Cu_9TlS_5+Cu_2S+CuS	53.28±0.69	44.23±3.99	30.36±11.38
Cu_3TlS_2+Cu_9TlS_5+CuS	48.56±0.49	38.46±2.79	33.90±8.07
CuTlS+ Cu_3TlS_2+ $CuTlS_2$	46.01±0.30	41.98±1.67	13.53±4.73

$CuTlS_2$+ CuS+S	54.69±0.01	55.96±0.68	-4.25±1.93

Table 5. Relative partial thermodynamic functions of copper in Cu-Tl-S alloys at 298 K

Phase area in Fig.1	$-\Delta\overline{G}_{Cu}$	$-\Delta\overline{H}_{Cu}$	$\Delta\overline{S}_{Cu}$
	кJ·mol^{-1}		J·mol^{-1}·K^{-1}
$CuTlS_2$+TlS_2+S	42.02±0.10	43.64±0.56	-5.40±1.64
CuTlS+$CuTlS_2$+Tl_4S_3	40.04±0.11	37.57±0.66	8.30±1.90
Cu_3TlS_2+$CuTlS_2$+ CuS	34.75±0.09	32.82±0.52	6.46±1.47
Cu_9TlS_5+Cu_3TlS_2+ CuS	33.20±0.08	28.18±0.50	12.93±1.38

The EMF isotherms of cells (6) and (7) along the Cu_2S-Tl_2S section are presented in Fig.2. As can you see, the EMF values of both types of cells is constant within a certain phase region and changes abruptly when moving from one phase region to another. In this case, the numerical values of the EMF increase with a decrease in the thallium concentration in the alloys. For cells (6) this is expected, but for cells (7) such a picture, at first view, contradicts the well-known requirement [43] that it is impossible to reduce the EMF value with a decrease in the concentration of the potential-forming component in the alloy. However, a comparison of Fig. 2 with the phase diagram (Fig. 1) shows that both dependences are in accordance with the above requirement, namely, the EMF values increase with decreasing concentration of the potential-forming component along the corresponding ray straight lines (red and blue lines in Fig. 1).

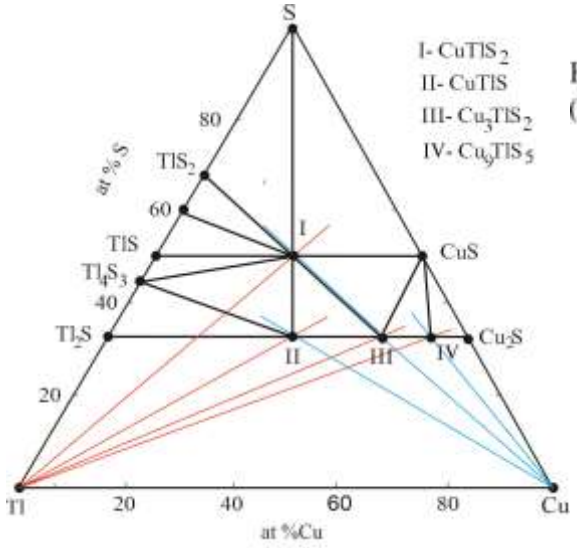

Fig.1. The solid-phase equilibria diagram of the Cu-Tl-S system at 300 K.

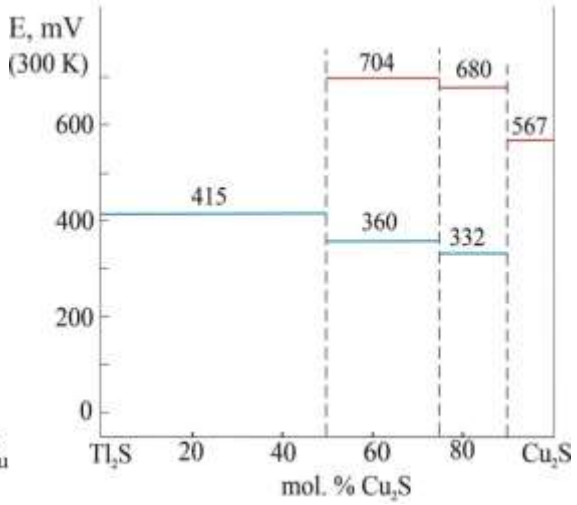

Fig.2. EMF isotherms of concentration cells (6) and (7) along the Cu_2S-Tl_2S section

The partial molar functions of thallium and copper (Tables 4 and 5) characterize various virtual potential formation reactions. According to the phase diagram (Fig. 1), the partial molar values of thallium in the indicated phase regions (Table 4) are the thermodynamic characteristics of the following potential formation reactions (all substances are in crystalline form):

$$Tl+CuS+S=CuTlS_2 \quad (8)$$
$$Tl+CuS+Cu_2S=Cu_9TlS_5 \quad (9)$$

$$Tl+CuS+\frac{1}{3}\ Cu_9TlS_5=\frac{4}{3}\ Cu_3TlS_2 \quad (10)$$

$$Tl+0.\ 5Cu_3TlS_2+0.5\ CuTlS_2=2CuTlS \quad (11)$$

Similarly, the partial molar functions of copper (Table 5) are the thermodynamic characteristics of the below potential formation reactions:

$$Cu+TlS_2=CuTlS_2 \quad (12)$$
$$Cu+0.25Tl_4S_3+0.25CuTlS_2=1.25CuTlS \quad (13)$$
$$Cu+0.5CuTlS_2=0.5Cu_3TlS_2 \quad (14)$$
$$Cu+0.333Cu_3TlS_2+CuS=0.333Cu_9TlS_5 \quad (15)$$

Using the above equations for potential formation reactions, the standard thermodynamic functions of formation and standard entropies of copper-thallium sulfides were calculated. For example, in accordance with reaction (8) for the $CuTlS_2$ compound, calculations were carried out using the relations

$$\Delta Z^0_{CuTlS_2}=\Delta\overline{Z}_{Tl}+\Delta Z^0_{CuS} \quad (16)$$

$$S^0_{CuTlS_2}=\Delta\overline{S}_{Tl}+S^0_{Tl}+S^0_{CuS} \quad (17)$$

(here $\Delta Z^0\equiv\Delta G^0$ or ΔH^0 of the corresponding compound, $\Delta\overline{Z}\equiv\Delta\overline{G}_{Cu}$ or $\Delta\overline{H}_{Cu}$) and taking into account reaction (12) according to the relations:

$$\Delta Z^0_{CuTlS_2}=\Delta\overline{Z}_{Cu}+\Delta Z^0_{TlS_2} \quad (18)$$

$$S^0_{CuTlS_2}=\Delta\overline{S}_{Cu}+S^0_{Cu}+S^0_{TlS_2} \quad (19)$$

In addition to the partial molar values of thallium or copper (Tables 4 and 5), thermodynamic data for the compounds TlS_2, Tl_4S_3 [110], Cu_2S and CuS [111] (Table 6), as well as standard entropies of copper (S^0_{298} =33.1±0.5 $J\cdot mol^{-1}\cdot K^{-1}$) and thallium ($S^0_{298}$ =64.18±0.21 $J\cdot mol^{-1}\cdot K^{-1}$) [112] were used for calculations equations (8)-(15).

The obtained two series of values of standard integral thermodynamic functions of copper-thallium sulfides are listed in Table 6.

Table 6. Standard integral thermodynamic functions of ternary compounds of the Cu-Tl-S system and some binary compounds used in calculations

Compounds	$-\Delta_fG^0(298K)$	$-\Delta_fH^0(298K)$	$S^0(298K)$	**Ref.**
	κJ·mol^{-1}		**J·mol^{-1}·K^{-1}**	
CuS	36.8±0.4	42.7±3.4	46.4±2.9	[111]
Cu_2S	66.1±0.8	63.2±5.9	108.8±5.4	[111]
TlS_2	52.3±0.5	50.0±0.8	145.0±0.9	[110]
Tl_4S_3	196.8±1.5	197.4±6.5	348.5±20.5	[110]
$CuTlS_2$	91.5±0.5	98.6±4.0	172.7±2.8	[108]
	94.3±0.7	93.6±1.4		[109]
CuTlS	84.1±1.5	82.1±4.9	132.4±6.2	[108]
	90.3±0.7	88.3±2.1		[109]
Cu_3TlS_2	152.7±1.8	145.8±12.3		[108]

	163.8±2.6	159.2±9.8	251.8±5.8	[109]
Cu_9TlS_5	354.6±4.5	339.7±30.8		[108]
	373.8±3.9	371.8±21.4	529.0±19.0	[109]

Table 6 shows that the values of the standard thermodynamic functions for the formation of ternary compounds obtained by two modifications of the EMF method are in satisfactory agreement with each other. This confirms the reversibility of the concentration cells of (6) and (7) types, and the reliability of thermodynamic data for copper and thallium sulfides [110,111], used by the authors [108, 109] in the calculations.

The Cu-Tl-Se system. The quasi-binary Cu_2Se-Tl_2Se section of this system is characterized by the formation of the ternary CuTlSe, $Cu_7Tl_3Se_5$, Cu_3TlSe_2, $Cu_8Tl_2Se_5$ and Cu_9TlSe_5 compounds [113]. According to [21], the CuTlSe-TlSe, CuTlSe-Tl and CuTlSe-Se sections are also quasi-binary. The first section forms a phase diagram of a simple eutectic type, the second section is related to a monotectic type, and the third one is characterized by the formation of an incongruently melting ternary $CuTlSe_2$ compound.

There is literature data about the synthesis and crystal structure of ten copper selenides with thallium [21, 114]. However, up to now, a complete picture of phase equilibria in the Cu-Tl-Se system has not been obtained. In [115], a fragment of the solid-phase equilibria diagram of this system was constructed, which reflected three ternary compounds (Fig. 3) and their thermodynamic properties were studied by the EMF method with a solid electrolyte. For the compounds $CuTlSe_2$ and CuTlSe, the corresponding thermodynamic data were previously obtained [43] by EMF measurements of (6) type cells (Table 7).

Table 7. Standard thermodynamic functions of formation and standard entropies of TlSe and some ternary phases of the Cu-Tl-Se and Cu-Tl-Te systems

Compounds	$-\Delta_f G^0(298K)$	$-\Delta_f H^0(298K)$	$S^0(298K)$,	Ref
	кJ·mol^{-1}		J·mol^{-1}·K^{-1}	
$CuTlSe_2$	96.29±0.16	97.91±0.95	176.1±5.1	[115]
	96.5±0.6	97.2±1.3		[43]
CuTlSe	84.49±0.16	81.37±0.85	149.9±2.8	[115]
	84.2±1.3	80.5±3.9		[43]
Cu_2TlSe_2	119.06±0.27	118.61±1.54	216.2±6.8	[115]
$CuTlTe_2$	75.1±0.4	72.6±1.3	208±4	[118]
Cu_2TlTe_2	99.2±0.5	94.3±2.1	249±6	[118]
	94.8±0.9	92±7	237±3	[119]
Cu_3TlTe_2	122.0±0.6	115.2±2.7	288±8	[118]
	117.1±1.2	117±5	263±4	[119]
Cu_9TlTe_5	264.3±2.6	253.8±9.8	637±15	[118]
	244.0±2.4	2431±14	621±7	[119]
$\delta(Cu_{0,2}Tl_{4,8}Te_3)$	210.2±1.7	213.0±2.2	454±7	[118]
$\delta(Cu_{0,4}Tl_{4,6}Te_3)$	207.8±1.6	210.5±2.3	449±7	[118]
$\delta(Cu_{0,6}Tl_{4,4}Te_3)$	205.3±1.6	207.6±2.4	444±8	[118]
$\delta(Cu_{0,8}Tl_{4,2}Te_3)$	203.8±1.5	206.0±2.5	438±8	[118]
$CuTl_4Te_3$	201.4±1.4	203.8±2.6	433±9	[118]

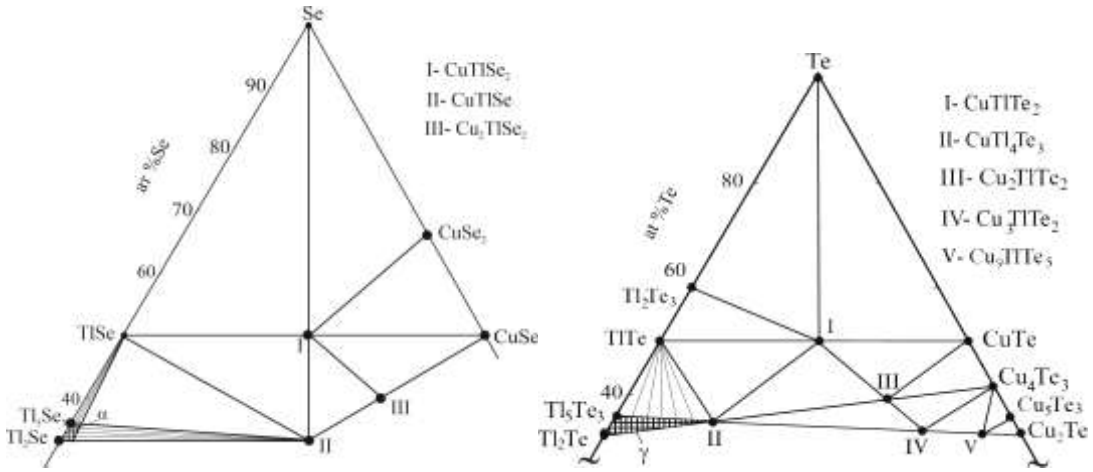

Fig. 3. Fragments of solid-phase equilibria diagrams of the Cu-Tl-Se [115] and Cu-Tl-Te [118] systems at 300 K.

The Cu-Tl-Te system. According to available data [21, 118], the Cu_2Te-Tl_2Te section is non-quasi-binary and is characterized by the formation of ternary Cu_9TlTe_5 and Cu_3TlTe_2 compounds with incongruent melting. Ternary compounds with the compositions $CuTlTe_2$, Cu_2TlTe_2 and $CuTl_4Te_3$ are also reported [21, 114, 116, 117].

The fragments of the Cu-Tl-Te solid-phase equilibria diagram and the results of a thermodynamic study of some copper-thallium tellurides by EMF measurements of concentration cells (6) and (7) are presented by authors of [118, 119]. Figure 3 shows the phase diagram at 300 K according to the data of [119], which reflects the above ternary compounds. The integral thermodynamic functions of three of them were determined by two modifications of the EMF method and are in satisfactory agreement (the discrepancies do not exceed 10%). Table 7 also shows thermodynamic data for $CuTl_4Te_3$-Tl_5Te_3 solid solutions [118].

4. Copper chalcogenides with p^2 elements

The most characteristic and studied copper chalcogenides with p^2- elements are compounds of the $Cu_2B^{IV}X_3$ and $Cu_8B^{IV}X_6$ types. Below is a brief overview of studies on the functional properties of these compounds.

Compounds of the $Cu_2B^{IV}X_3$ type, especially Cu_2SnSe_3, Cu_2GeSe_3, and alloys based on them have been widely studied as environmentally friendly and affordable thermoelectric materials [120-130]. It has been shown that Cu_2SnSe_3 doped with various elements (In, Zn, Ag, Sb, Pb, S, Te) [123, 124, 126, 129], as well as its composites with graphene and other phases [125, 128, 130], demonstrate good thermoelectric indicators. The thermoelectric characteristics of Cu_2GeSe_3 doped with various elements [121, 129], as well as solid solutions based on it [122] also improve.

Studies have shown that $Cu_2B^{IV}X_3$ compounds are also promising for use as photovoltaic and optoelectronic materials [131-144]. The photoelectric and optical properties of the Cu_2SnS_3 compound and alloys based on it have been studied in most detail [136-144]. Authors of [134] presents a review of works on the synthesis, structural transformation, morphological engineering and restructuring of the energy gap of nanoparticles of Cu–Sn–S(Se) systems and discusses the prospects for the development of solar cells based on them. In addition, other photovoltaic applications such as photoelectrocatalytic hydrogen production and dye degradation of Cu–Sn–S(Se) nanoparticles are also noted.

Another review [144] shows that the Cu_2SnS_3 ternary compound, consisting of non-toxic and readily available elements, is the preferred photovoltaic material for solar cell applications due to its optimal structural and optical properties. This paper also discusses the issues of efficiency loss in solar cells based on this compound and possible ways to eliminate them.

Copper-containing compounds of the

argyrodite family with the general formula $Cu_8B^{IV}X_6$ are also of great interest as effective ionic conductors, thermoelectric, photoelectric and nonlinear optical materials [145].

Cu argyrodites, being typical superionic semiconductors with two independent structural units (a rigid anionic framework and weakly bound Cu^+ cations), can serve as very good base compounds for the development of high-performance thermoelectric materials by separately tuning the electrical and thermal properties [145, 146]. It should be noted that only a small part of the research of the thermoelectric properties of argyrodites is devoted to the study of compounds of stoichiometric composition [146-148]. Most of the existing works on argyrodite thermoelectrics are focused on the production of nano- and single crystals, thin films, high-density polycrystals, complex phases, and composite materials based on them [145, 146, 149-151]. To increase thermoelectric efficiency, researchers often vary the composition of argyrodite compounds in the following ways [145]: 1. Complicating the composition through various types of substitution with analogue atoms; 2. Adding dopants; 3. Creation of a deficiency of individual elements in the stoichiometric composition.

The optical properties of some $A^I_8B^{IV}X_6$ compounds were studied in [152, 153]. It was shown [152] that replacing Ag with Cu in isostructural $A^I_8B^{IV}X_6$ compounds causes a clear increase in secondary harmonic generation. This result opens up the possibility of synthesizing high-quality infrared nonlinear optical materials based on them. Authors of [153] report the preparation of Cu_8SiS_6 and Cu_8SiSe_6 thin-film layers for optoelectronic applications.

4.1. The Cu-Si-X systems

Phase equilibria in the Cu-Si-S-Se ternary systems were studied along quasi-binary Cu_2S-SiS_2 [154] and Cu_2Se-$SiSe_2$ sections [155]. According to these works, copper and silicon form ternary compounds of the Cu_8SiX_6 and Cu_2SiX_3 compositions. The thermodynamic properties of these compounds have been practically not studied. There are works [68-70] in which the functions of phase transitions of some compounds were determined by the DSC method. These data are given in subsection 4.2. (Table 10).

4.2. The Cu-Ge-X systems

The Cu-Ge-S system. According to [156, 157], the Cu_2S-GeS_2 quasi-binary section is characterized by the formation of Cu_8GeS_6 and Cu_2GeS_3 compounds with incongruent melting at 1253 and 1213 K. Cu_8GeS_6 undergoes a polymorphic transformation at 328 K. An isothermal section of the phase diagram of the Cu-Ge-S system at 300 K (Fig. 4), at which the above ternary compounds were reflected is presented in [21].

The Cu-Ge-Se system. According to [158], the nature of phase equilibria along the Cu_2Se-$GeSe_2$ section is similar to the sulfide system: ternary compounds Cu_8GeSe_6 and Cu_2GeSe_3 melt with decomposition by peritectic reactions at 1080 K and 1037 K. The presented in [159] T-x diagram confirms Cu_2GeSe_3 compound with congruent melting at 1033 K, but instead of Cu_8GeSe_6 a compound of similar composition Cu_6GeSe_5 is presented. Later, this system was re-studied in the composition range of 15-60 mol% $GeSe_2$ [160] and it was shown that the congruent melting temperature of Cu_2GeSe_3 is 1053 K, and Cu_8GeSe_6 melts with decomposition at 1083 K and has a polymorphic transformation at 328 K.

The Cu-Ge-Te system studied in a number of works, the results of which are summarized in [21]. There is one ternary compound Cu_2GeTe_3 in the system.

Fig. 4 shows the phase diagrams of the Cu-Ge-S, Cu-Ge-Se and Cu-Ge-Te systems at room temperature [21]. The thermodynamic properties of copper-germanium chalcogenides were studied in [45, 161-163, 167] by EMF measurements of concentration cells of type (7).

When planning experiments on the Cu-Ge-S and Cu-Ge-Se systems, the authors of [161] proceeded from the fact that the Cu_8GeS_6 and Cu_8GeSe_6 compounds have polymorphic transitions in the temperature range of EMF measurements. Experiments have shown that the temperature dependences of the EMF for electrode alloys containing the Cu_8GeS_6 and Cu_8GeSe_6 compounds have the form of two straight lines with a break point at the temperature of their polymorphic transformation (Fig. 5). From the EMF measurements data, the partial molar functions of copper were

calculated for two modifications of the indicated compounds (Table 8), which were used to calculate the thermodynamic functions of formation (Table 9) and polymorphic transitions (Table 10).

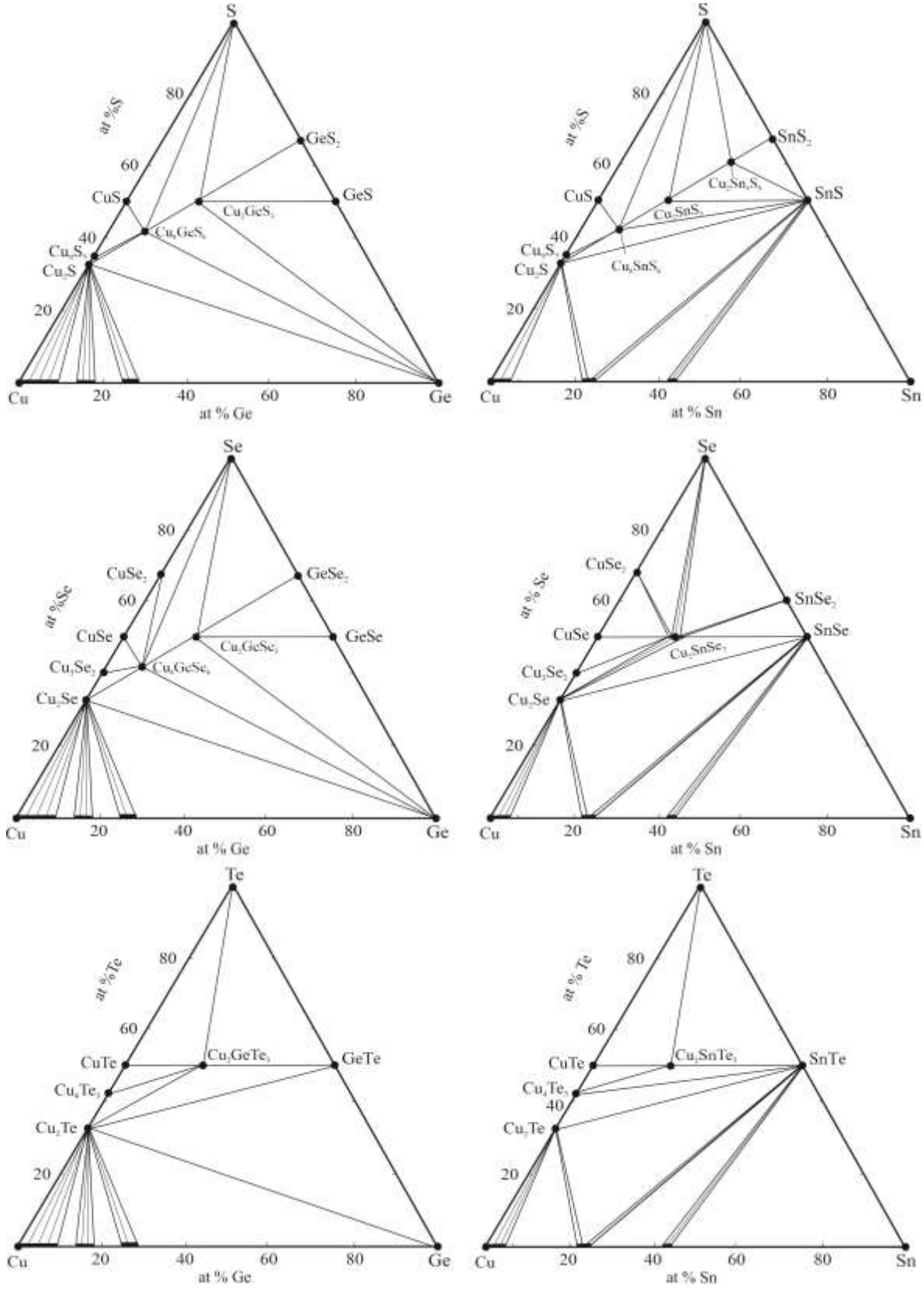

Fig.4. Solid-phase equilibria diagrams of Cu-Ge-X and Cu-Sn-X systems at 300 K [21].

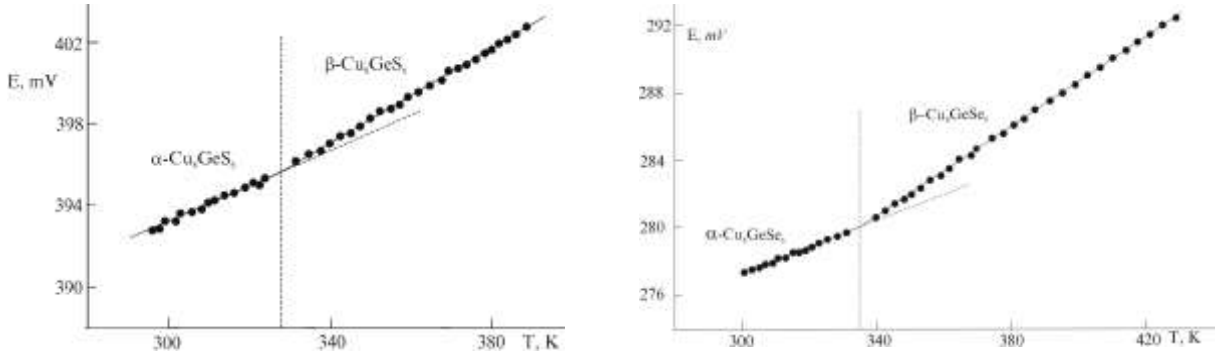

Fig.5. EMF dependences of concentration cells (7) for Cu_8GeS_6 and Cu_8GeSe_6 compounds [161]

Table 8. Partial molar thermodynamic functions of copper in some phase regions of the Cu-Ge-S and Cu-Ge-Se systems [161]

Phase area	T, K	$-\overline{\Delta G}_{Cu}$	$-\overline{\Delta H}_{Cu}$	$\overline{\Delta S}_{Cu}$
		κJ·mol^{-1}		J·mol^{-1}·K^{-1}
α-Cu_8GeS_6+Cu_2GeS_3+S	298	37.925±0.013	35.37±0.32	8.56±1.04
β-Cu_8GeS_6+Cu_2GeS_3+S	400	-39.000±0.098	34.52±0.55	11.19±1.52
α-Cu_8GeSe_6+Cu_2GeSe_3+Se	298	26.735±0.009	24.59±0.19	7.20±0.59
β-Cu_8GeSe_6+Cu_2GeSe_3+Se	400	27.856±0.059	22.61±0.27	13.12±0.70

Table 9. Standard integral thermodynamic functions of the argyrodite family compounds

Phase	$-\Delta_f G^0$	$-\Delta_f H^0$	S^0	**Ref.**
	κJ·mol^{-1}		**J·K^{-1}·mol^{-1}**	
Cu_2GeS_3	211.3±2.4	213.7±2,3	190.3±5.5	[167]
RT-Cu_8GeS_6	438.9±2.5	425.9±4.2	536.3±13.1	[161]
HT-Cu_8GeS_6	*445.3±3.1	420.8±5.6	552.1±15.8	[161]
Cu_2GeSe_3	178.4±18.8	174.5±19.7	223.4±6.6	[45]
	176.8±3.1	173.9±3.1	233.3±5.1	[162]
RT- Cu_8GeSe_6	341.1±3.3	327.4±4,5	596.7±11.6	[161]
	105.1±1.9	114.5±9.2	143±2	[162]
HT- Cu_8GeSe_6	*348.1±3.7	315.6±5.0	632.3±12.5	[161]
$Cu_2Sn_4S_9$	659.9±4.3	650.9±29.7	560.3±74.7	[45]
	165.4±1.5	141.6±6.3	639.8±18.3	[165]
Cu_2SnS_3	239.6±1.5	242.6±12.0	196.3±21.9	[45]
	169.3±1.3	150.0±5.5	278.6±15.7	[165]
Cu_4SnS_4	316.4±2.4	327.7±18.8	266.5±28.2	[45]
	261.3±2.4	220.8±9.4	414.4±20	[165]
Cu_2SnSe_3	189.5±2.6	187.5±4.8	251.6±5.0	[45,166]
	198.4±0.6	198.5±2.9	237±5	[43]
Cu_2SnTe_3	117.7±1.4	116.2±2.4	264±6	[45]

***Note:** data at 400 K is marked with an asterisk.

In [161], the thermodynamic functions of the polymorphic transformations of the Cu_8GeS_6 and Cu_8GeSe_6 compounds were calculated from EMF measurements data. Let us consider the method of these calculations using Cu_8GeS_6 as an example. Since in the temperature range of EMF measurements the heat of formation of this compound is almost constant, then

$$\Delta H_{p.t.} = \Delta_f H^0(\beta) - \Delta_f H^0(\alpha) \ . \quad (20)$$

where $\Delta H_{p.t.}$ - is the heat of polymorphic transformation; $\Delta_f H^0(\beta)$ and $\Delta_f H^0(\alpha)$ - are the heats of formation of two modifications of this compound. On the other hand, from following relation

$$6Cu+Cu_2GeS_3+3S=Cu_8GeS_6 \quad (21)$$

it follows that the contribution of Cu_2GeS_3 to the $\Delta_f H^0(\beta)$ and $\Delta_f H^0(\alpha)$ functions is the same. Therefore, the calculation of $\Delta H_{p.t.}$ was carried out according to the relation

$$\Delta H_{p.t.} = 6[\Delta \overline{H}_{Cu}(\beta) - \Delta \overline{H}_{Cu}(\alpha)]. \quad (22)$$

which does not include the value and error of the heat of formation of Cu_2GeS_3.

The entropy of the polymorphic transformation is calculated using the relation

$$\Delta S_{p.t.} = \Delta H_{p.t.} / T_{p.t.} \quad (23)$$

Table 10 shows the thermodynamic functions of phase transitions of these compounds and their silicon analogues, obtained by the DSC method [69, 70, 164]. Table 10 demonstrates that the data obtained by both methods (exception for the Cu_8GeS_6) are in good agreement. Calorimetric data is more accurate. Relatively high errors in the data obtained by the EMF method are due to the fact that in this method partial enthalpy and entropy are calculated indirectly from the temperature dependence coefficient of the EMF [42, 43].

Table 10. Temperatures and thermodynamic functions of phase transitions of some $Cu_8B^{IV}X_6$ compounds

Compound	$T_{p.t.}$	$\Delta H_{p.t.}$, kJ·mol^{-1}	$\Delta S_{p.t..}$, J·mol^{-1}·K^{-1}	Method, Ref.
Cu_8GeS_6	328	5.1±2.4	15.5±7.5	EMF, [161]
	330	15.54±0.62	47.09±1.88	DSC, [70]
Cu_8GeSe_6	335	11.9±2.8	35.5±8.4	EMF, [161]
	330	11.23±0.45	34.03±1.36	DSC, [164]
Cu_8SiS_6	336	14.85±0.59	44.20±1.77	DSC, [70]
Cu_8SiSe_6	325	14.73±0.59	45.32±1.81	DSC,[69]

4.3. The Cu-Sn-X systems

The Cu-Sn-S system. Some polythermal sections of this system were studied in the 70s of the last century and summarized in [21]. It is shown that the Cu_2S-SnS and Cu_2S-SnS_2 sections are quasi-binary. The first belongs to the eutectic type, and in the second 4 intermediate phases are formed: Cu_2SnS_3, Cu_4SnS_4, $Cu_4Sn_3S_6$, and $Cu_2Sn_4S_9$. The isothermal section of the phase diagram at 300 K (Fig. 4), presented in [21], reflects the above copper-tin sulfides.

The Cu-Sn-Se system. The only ternary compound of this system, Cu_2SnSe_3, is formed on the quasi-binary Cu_2Se-$SnSe_2$ section and melts congruently at 963 K [21]. The T-x-y diagram and isothermal section of the phase diagram at 300 K (Fig. 4) based on data from a number of works were constructed in [21].

The Cu-Sn-Te system. In [21], a complete T-x-y diagram of this system is presented, characterized by the presence of one ternary compound Cu_2SnTe_3. This compound has a cubic structure and melts incongruently at 680 K.

The thermodynamic properties of copper-tin chalcogenides were studied by the EMF method with a solid electrolyte [45, 165, 166],

and the Cu_2SnSe_3 compound was also studied by the classical version of the EMF method with a liquid electrolyte. From the measurement data of the EMF of cells of type (7) using relations (3)-(5), the partial molar functions of copper in the alloys were calculated. The authors employed solid-phase equilibrium diagrams of the corresponding systems (Fig. 4) to calculate the integral thermodynamic functions. Table 9 show that the thermodynamic functions of Cu_2SnSe_3 obtained by two modifications of the EMF method are in good agreement with each other. It is also clear from Table 9 that the numerical values of the thermodynamic functions of copper-tin sulfides according to [165] are significantly lower than the data from [45]. For the compounds $Cu_2Sn_4S_9$ and Cu_4SnS_4, the data [165] are even lower than the sum of the corresponding values for Cu_2S and SnS_2, which is thermodynamically impossible. It was noted in [21] that this is the result of incorrect definition of potential-forming reactions by the authors of [165].

4.4. Quaternary systems including chalcogenides of copper and p^2-elements

In the last decade, in order to search for solid solutions with various types of substitutions based on copper chalcogenides with p2 elements, some quasi-ternary (Cu_2S-Ag_2S-GeS_2 [168], Cu_2Se-Ag_2Se-$GeSe_2$ [168], Cu_2Se-$GeSe_2$-$SnSe_2$ [169], Cu_2S-Cu_8SiS_6-Cu_8GeS_6 [70], Cu_2Se-Cu_8SiSe_6-Cu_8GeSe_6 [170]) and reciprocal ($2Cu_2S+GeSe_2 \leftrightarrow 2Cu_2Se+GeS_2$ [171, 172], $2Cu_2S+SnSe_2 \leftrightarrow 2Cu_2Se+SnS_2$ [168]) systems.

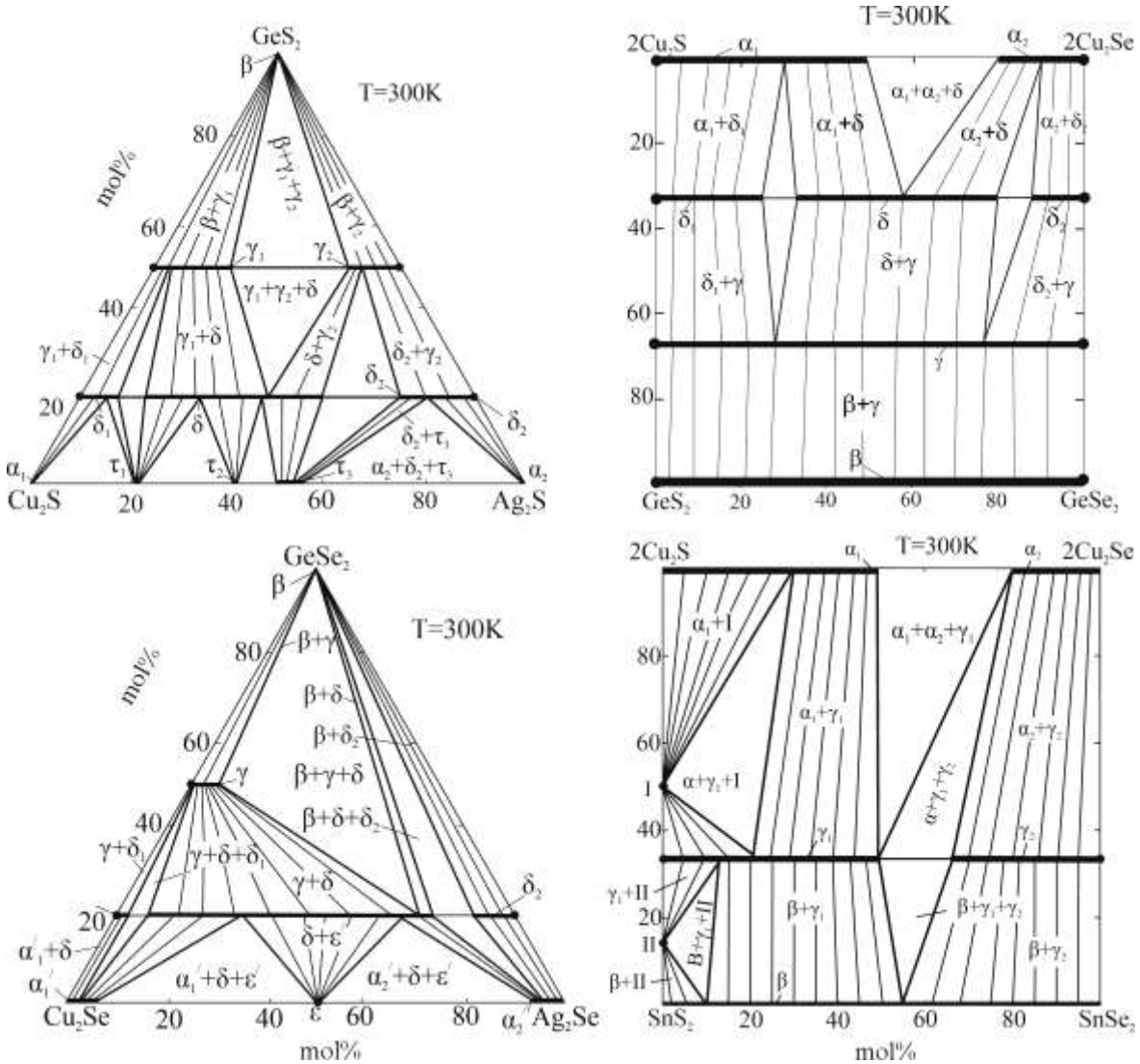

Fig.6. Solid-phase equilibria diagrams of quasi-ternary Cu_2S-Ag_2S-GeS_2 Cu_2Se-Ag_2Se-$GeSe_2$ and reciprocal $2Cu_2S+GeSe_2 \leftrightarrow 2Cu_2Se+GeS_2$ и $2Cu_2S+SnSe_2 \leftrightarrow 2Cu_2Se+SnS_2$ systems

Isothermal sections of phase diagrams at room temperature (Fig. 6) clearly demonstrate the formation of unlimited or broad solid solutions based on ternary compounds. A number of works [70, 167-169, 172-175] present the results of a comprehensive study of phase equilibria and thermodynamic properties of the above and some similar systems.

As an example, let's consider Cu_2S-Ag_2S-GeS_2 system [167]. The results of EMF measurements of concentration chains of type (7) were in accordance with the solid-phase equilibrium diagram (Fig. 6) and confirmed the formation of wide areas of solid solutions based on Cu_2GeS_3 and Ag_2GeS_3 compounds. The concentration dependence curves of EMF (Fig. 7) and partial molar functions of copper at 298 K (Fig. 8) have a form which is characteristic for systems with the formation of limited solid solutions based on the starting compounds. Within the homogeneity region of α- and β-solid solutions based on Cu_2GeS_3 and Ag_2GeS_3, respectively, the partial molar functions of copper are monotonic functions of composition, and in the heterogeneous α+β region have constant values, since the compositions of the coexisting phases are almost constant.

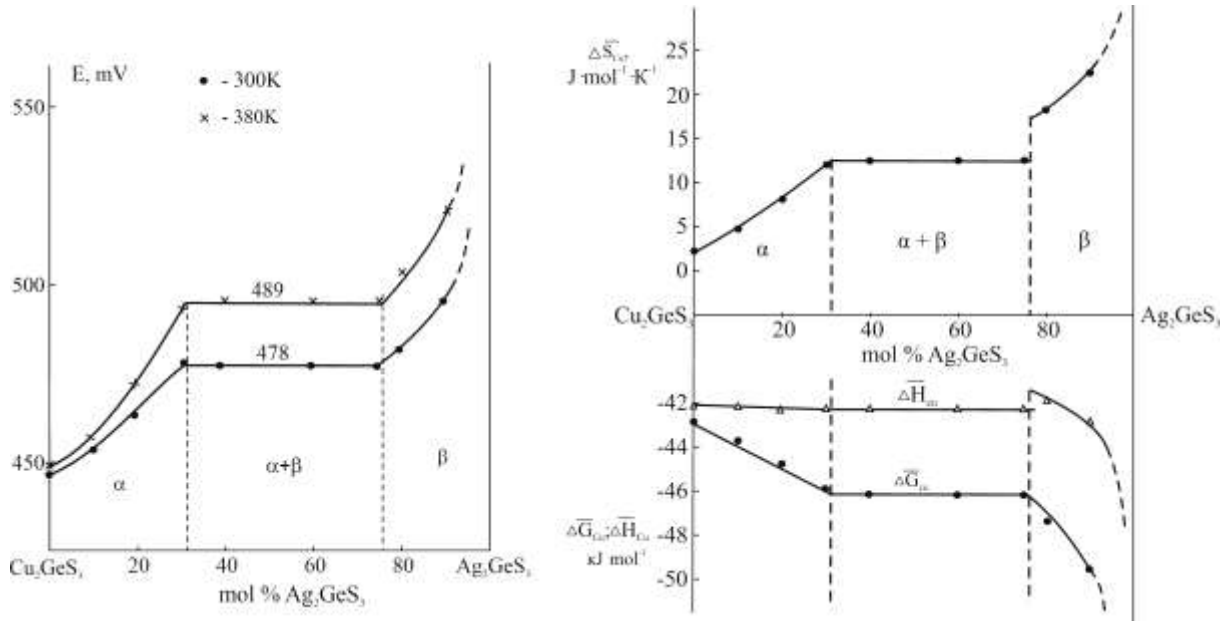

Fig.7. Isotherms of EMF of cells of type (7) and partial molar functions of copper in the Cu_2GeS_3-Ag_2GeS_3 system

Based on the analysis of the Cu-Ag-Ge-S concentration tetrahedron (Fig. 8), the authors of [167] determined potential-forming reactions for individual compositions of $Cu_{2-x}Ag_xGeS_3$ solid solutions. As can be seen, the ray lines from the top of Cu, passing through the Cu_2GeS_3-Ag_2GeS_3 section, reach the concentration plane of the side ternary system Ag-Ge-S in the three-phase region Ag_2GeS_3+GeS_2+S. Therefore, in the overall potential-forming reaction for $Cu_{2-x}Ag_xGeS_3$ solid solutions, the phases of the indicated three-phase region and elemental copper must interact. For example, for a solid solution with $Cu_{0.2}Ag_{1.8}GeS_3$ composition the potential-forming reaction has following form:

$$Cu+4.5Ag_2GeS_3+0.5GeS_2+0.5S= 5Cu_{0.2}Ag_{1.8}GeS_3,$$

and the relations for calculating its integral thermodynamic functions ($\Delta Z \equiv \Delta G$ or ΔH) as below:

$$\Delta_f Z^0=0.2\Delta\bar{Z}_{Cu}+0.9\Delta_f Z^0(Ag_2GeS_3)+0.1\Delta_f Z^0(GeS_2)$$
$$S^0=0.2\Delta\bar{S}_{Cu}+0.2S^0(Cu)+0.9S^0(Ag_2GeS_3)+0.1S^0(GeS_2)+0.1S^0(S)$$

In a similar way, the standard integral thermodynamic functions of $Cu_{2-x}Ag_xGeS_3$ solid solutions were calculated for x = 0.4; 0.6; 1.6; 1.8 compositions. The results are presented in Table 11.

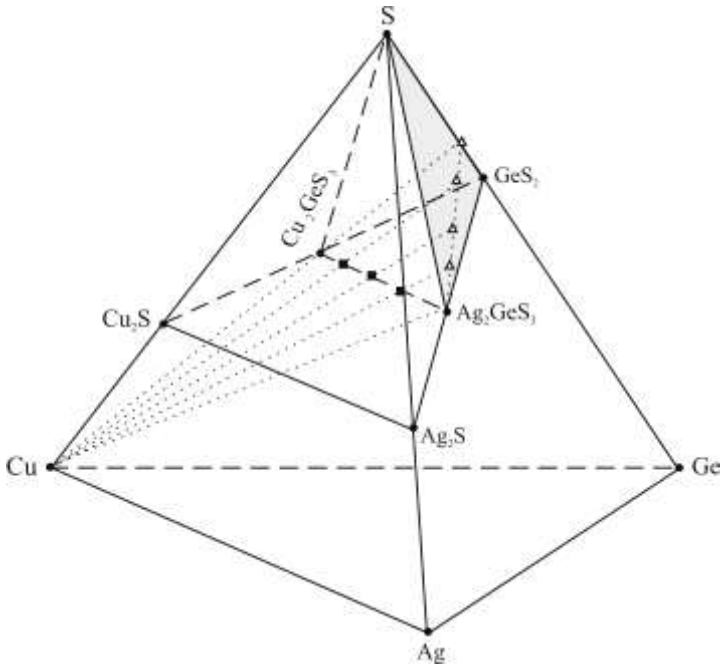

Fig.8. For calculation of integral thermodynamic functions of phases in the Cu_2GeS_3- Ag_2GeS_3 system

Table 11. Standard integral thermodynamic formation functions and standard entropies of the Cu_2GeS_3 and Ag_2GeS_3 compounds and $(Cu_2GeS_3)_x(Ag_2GeS_3)_{1-x}$ solid solutions [167]

Composition	$-\Delta_fG°(298K)$	$-\Delta_fH°(298K)$	$S°(298K)$
	$kJ·mol^{-1}$		$J·K^{-1}·mol^{-1}$
Cu_2GeS_3	211.3±2.4	213.7±2.3	190.3±5.5
$(Cu_2GeS_3)_{0.9}(Ag_2GeS_3)_{0.1}$	212.2±2.1	210.7±2.2	199.9±5.2
$(Cu_2GeS_3)_{0.8}(Ag_2GeS_3)_{0.2}$	213.3±2.1	209.6±2.2	209.4±5.7
$(Cu_2GeS_3)_{0.7}(Ag_2GeS_3)_{0.3}$	214.0±2.1	208.2±2.2	219.1±5.8
$(Cu_2GeS_3)_{0.2}(Ag_2GeS_3)_{0.8}$	208.9±2.1	200.7±2.2	235.8±8.0
$(Cu_2GeS_3)_{0.1}(Ag_2GeS_3)_{0.9}$	207.4±2.1	199.6±2.2	238.3±8.3
Ag_2GeS_3	206.0±2.1	198.0±2.2	239.1±8.8

5. Copper chalcogenides with arsenic subgroup elements

Cu-As(Sb)-chalcogen systems attract close attention of researchers for two reasons. Firstly, the compounds of these systems and phases based on them are valuable environmentally friendly functional materials with photoelectric, optical [176-192] and thermoelectric [193-202] properties. Secondly, many known ternary compounds of these systems occur in nature in the form of minerals: enargite and lucionite Cu_3AsS_4; tennantite $Cu_{12}As_4S_{31}$, tetrahedrite $Cu_{12}Sb_4S_{31}$; chalcostibite $CuSbS_2$; synnergite $Cu_6As_4S_9$; lautite CuAsS, etc. These mineral compounds are of great interest for mineralogy and geochemistry and provide valuable information about the physical conditions on Earth at the time of their occurrence [36, 37].

Copper-arsenic (antimony) sulfides [176-192] are considered promising candidates for use as *p*-type absorbers in solar cells due to the wide availability and environmental friendliness of the raw material, suitable band gap and high absorption coefficient. The suitable band gap of

these phases indicates the prospect of their application also as wide-bandgap semiconductors in third-generation photovoltaic devices. The largest number [184-191] of works is devoted to chalcostibite $CuSbS_2$, which is considered as a substitute material for $CuInS_2$ due to its similar optical properties and the additional advantage of a higher content of antimony in the Earth and its lower cost compared to indium.

Synthetic analogues of multiple copper minerals [193-198], as well as solutions and composites based on them [198-202] have low thermal conductivity and an anistropic crystal structure and exhibit promising thermoelectric properties. Thus, in review [198], it was noted that by 2015, zT values of the order of ~1.0 at ~723 K were achieved for a number of natural and doped tetrahedrite materials, which is comparable to conventional *p*-type thermoelectric materials. The authors of [202] proposed a new concept for increasing the stability and efficiency of copper thermoelectrics, which consists in producing composites of the "copper chalcogenide-copper tetrahedrite" type. According to these authors, the proposed solution can successfully block excessive migration of copper and stabilize the composition and properties of the material during subsequent thermal cycles.

It should also be noted that, according to a number of studies, copper-bismuth chalcogenides, in particular $CuBiS_2$, demonstrate good photothermal properties and an anticancer effect [34]. Due to their high X-ray attenuation coefficient, these compounds have the ability to visualize computed tomography [35].

5.1. The Cu-As-X systems

The Cu-As-S system. Numerous works on phase equilibria and properties of ternary phases in the Cu–As–S system covering the period until the early 90s of the last century are summarized in [21, 203]. It is shown that the available data on the Cu_2S-As_2S_3 phase diagram section are contradictory and differ from each other both in the number and composition of ternary compounds, and in the temperatures and nature of their melting. In particular, it was shown in [204] that this system is quasi-binary and is characterized by the formation of ternary compounds Cu_5AsS_4, Cu_3AsS_3, $Cu_{12}As_4S_{13}$, $Cu_4As_2S_5$ and $Cu_6As_4S_9$. The authors of [203], taking into a number of studies, presented a slightly different version of the phase diagram from [204], according to which there are 3 ternary compounds in the system: $Cu_{12}As_4S_{13}$, $Cu_4As_2S_5$ and $Cu_6As_4S_9$. It should be noted that the composition of the $Cu_{12}As_4S_{13}$ phase is outside the plane of this section, which casts doubt on the data [203] on its quasi-binarity. [205] presented a new review of the literature on the Cu–As–S system and carried out a critical assessment and thermodynamic modeling of the phase diagram.

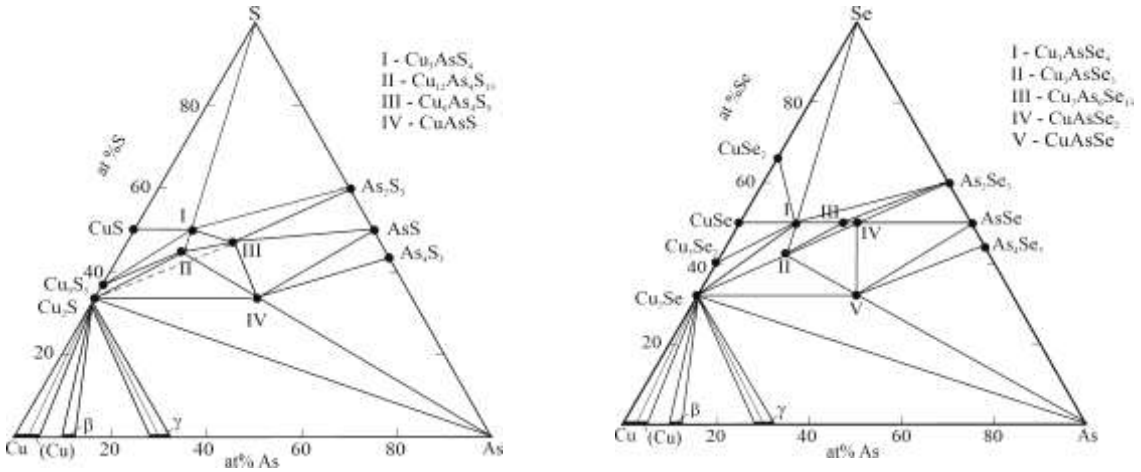

Fig. 9. Diagrams of solid-phase equilibria for the Cu-As-S and Cu-As-Se systems

The studies [206-209] published by our research team the results of a comprehensive study of phase equilibria and thermodynamic properties of the Cu-As-S system were

presented. The solid-phase equilibrium diagram (Fig. 9) shows ternary Cu_3AsS_4, $Cu_{12}As_4S_{13}$, $Cu_6As_4S_9$ and CuAsS compounds.

Table 12. Standard thermodynamic functions of formation and standard entropies of the ternary phases of the Cu-As-S(Se) systems

Compound	$-\Delta_f G^0(298K)$	$-\Delta_f H^0(298K)$	$S^0(298K)$,	Ref.
	κJ·mol^{-1}		J·K^{-1}·mol^{-1}	
Cu_3AsS_4 (enargite)	179.2±0.6	172.2±2.6	278±8	[208, 209]
	211.6	215.7	276.6	[216]
	230.4	224.0	285.0	[205]
		179.0	256.4	[37]
			277.2	[217]
$Cu_6As_4S_9$ (synnerite)	445.3±1.6	434.6±7.5	668±22	[208, 209]
	517.8	505.1	673.0	[205]
$Cu_{12}As_4S_{13}$ (tennantite)	701.8±2.5	673.7±10.7	1050±13	[208, 209]
CuAsS (lautite)	69.5±0.3	64.1±1.7	109±5	[208, 209]
	76.2	76.5	100.0	[205]
Cu_3AsSe_4	147.3±0.5	146.3±1.5	307±13	[213]
$Cu_7As_6Se_9$	441.8±2.3	446.1±11.7	970±27	[59]
$CuAsSe_2$	61.1±0.4	62.1±1.9	149.5±4.5	[215]
	66.6±0.4	67.33±2.0	150.9±6.2	[215]
Cu_3AsSe_3	141.8±0.5	140.0±2.0	258.5±5.6	[59]
CuAsSe	55.1±0.3	55.6±2.0	109.5±4.7	[59]

The Cu-As-Se system. Phase equilibria in this system have been studied in detail along the quasi-binary Cu_2Se-As_2Se_3 section [21, 210, 211]. According to [210], the Cu_3AsSe_3 and $CuAsSe_2$ compounds are formed in the system. Authors of [211] show the formation of the Cu_3AsSe_3, $Cu_4As_2Se_5$ and $CuAsSe_2$ ternary compounds.

The studies [45, 212-215] present the results of studying the phase equilibria and thermodynamic properties of the Cu-As-Se system. It has been established that it is characterized by the presence of ternary compounds Cu_3AsSe_3, $Cu_7As_6Se_9$, $CuAsSe_2$, Cu_3AsSe_4 and CuAsSe (Fig. 9).

The Cu-As-Te system. According to available data [21], no ternary compounds are formed in this system.

Table 12 shows the standard integral thermodynamic functions of copper-arsenic chalcogenides. The data sets obtained by the EDS method [208, 209] for Cu_3AsS_4, $Cu_6As_4S_9$, and CuAsS are significantly (up to 20%) lower than those given in [205] and are closer to the data in [37, 216]. The standard entropy values presented in various papers are consistent with each other. Unfortunately, the data [37, 205, 216, 217] are presented without errors, which makes it difficult to assess their reliability. We believe that the data from [205] are greatly overestimated.

5.2. The Cu-Sb-X systems

The Cu-Sb-S system. Research of phase equilibria in the Cu-Sb-S system began at the beginning of the last century. The results of numerous studies in different years were summarized in the monograph [21] and papers [218, 219]. Phase equilibria of the Cu−S−Sb system are calculated in the recently published work [220] utilizing the CALPHAD (CALculation of PHAse Diagrams) technique and a new version of the T-diagram of the Cu_2S-Sb_2S_3 section was presented. This diagram significantly different from previous reports.

The complete T-x-y diagram and various sections of the phase diagram, including the isothermal section at 300 K (Fig. 10), are presented by us in [221, 222]. According to their data, the system contains ternary compounds Cu_3SbS_4, $Cu_{12}Sb_4S_{13}$, $Cu_{14}Sb_4S_{13}$,

Cu_3SbS_3 and $CuSbS_2$, in addition, the Cu_2S-Sb_2S_3 cut, in contrast to the literature data, is non-quasi-binary.

Table 13. Standard thermodynamic functions of formation and standard entropy of some ternary copper –antimony (bismut) chalcogenides

Compound	$-\Delta_f G^0(298K)$	$-\Delta_f H^0(298K)$	$S^0(298K)$, $J\cdot K^{-1}\cdot mol^{-1}$	Ref.
	$kJ\cdot mol^{-1}$			
Cu_3SbS_4	254.7 ± 2.3	247.8 ± 2.3	295.6 ± 7.0	[221]
$CuSbS_2$	128.5 ± 2.2	126.9 ± 2.4	147.5 ± 3.8	[221]
	*132.7±4.2	130.8±4.4	-	[223]
	130.6±6.0	131.7±5.2	-	[224]
$Cu_{12}Sb_4S_{13}$	958.7 ± 9.6	929.7 ± 11.2	1092.0 ± 29.0	[221]
Cu_3SbS_3	226.4 ± 2.3	219.0 ± 2.6	265.5 ± 7.2	[221]
	*221.6±6.0	215.0±6.2	-	[223]
$Cu_{14}Sb_4S_{13}$	971.7 ± 9.8	984.8 ± 11.9	1018.0 ± 33.0	[221]
Cu_3SbSe_4	191.6±2.5	178.6±5.4	358.18	[59]
$CuSbSe_2$	101.4±1.8	98.5±2.2	173±8	[59]
	77.3±1.3	104.8±1.7	-	[224]
Cu_3SbSe_3	175.6±2.5	164.0±5.3	311±15	[59]
$CuBiS_2$	138.6±4.0	138.2±2.9	156±12	[45]
Cu_3BiS_3	213.0±4.4	209.9±5.2	264±21	[45]
$CuBi_3S_5$	248.7±1.9	248.6±5.8	421.9±7.8	[45]
$CuBiSe_2$	107.6±0.8	105.9±2.51	189.8±2.4	[225]
Cu_3BiSe_3	162.5±1.2	155.9±5.7	315.0±8.5	[225]
Cu_9BiSe_6	324.8±3.5	313.1±18.6	659±28	[225]

Note: * - our calculation from calorimetric data [223].

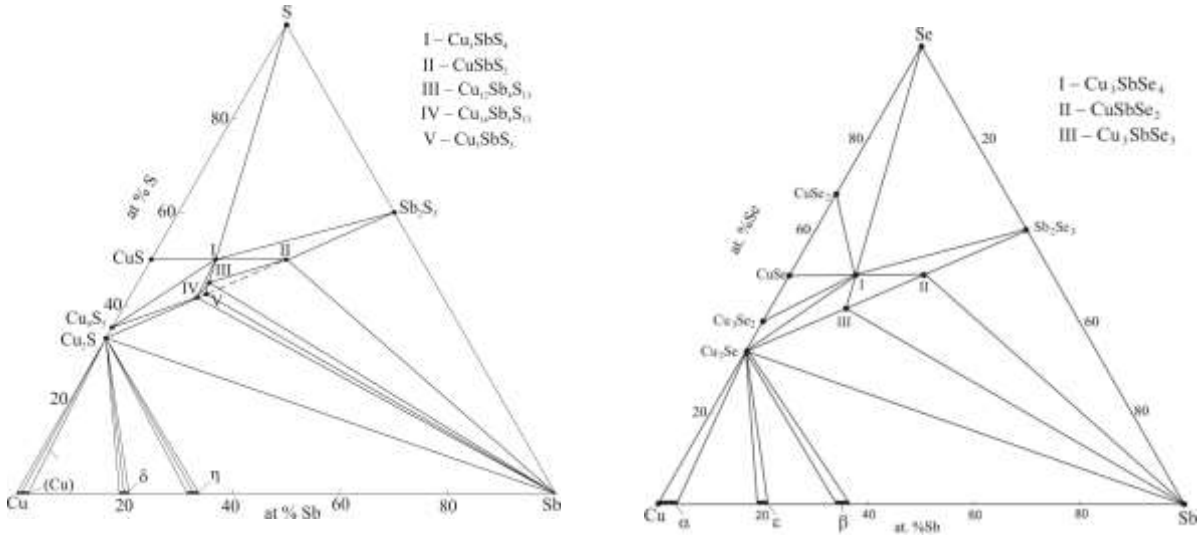

Fig. 10. Diagrams of solid-phase equilibria of the Cu-Sb-S and Cu-Sb-Se systems

The Cu-Sb-Se system is characterized by the formation of ternary compounds Cu_3SbSe_4, $CuSbSe_2$ and Cu_3SbSe_3 [21] (Fig. 10). The first two compounds melt congruently, and the third one melts incongruently via a peritectic reaction.

The Cu-Sb-Te system. According to available data [21], no ternary compounds are formed in this system. The compound $CuSbTe_2$ indicated in some early studies was not

subsequently confirmed.

5.3. The Cu-Bi-X systems

The Cu-Bi-S system. Phase equilibria in this system have been studied in numerous studies over more than 100 years. A review of the available data is given in [21, 219]. According to the solid-phase equilibrium diagram, the following copper-bismuth sulfides exist at room temperature: $CuBi_3S_5$, $CuBiS_2$ and Cu_3BiS_3 (Fig. 11).

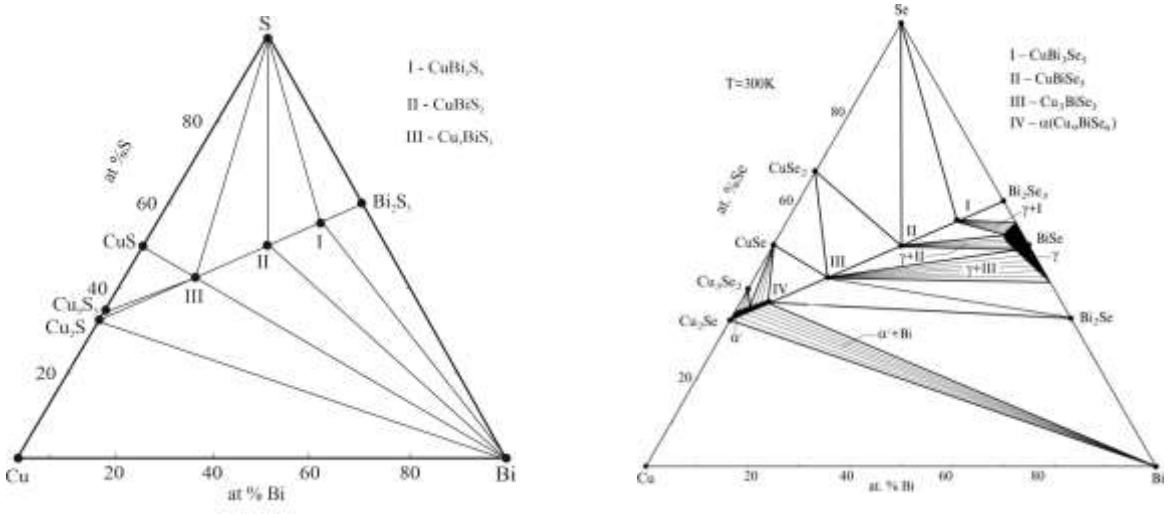

Fig. 11. Solid-phase equilibrium diagrams of Cu-Bi-S(Se) systems

The Cu-Bi-Se system. The paper [225] summarizes the results of all available studies on phase equilibria and presents a complete picture of phase equilibria, including the liquidus surface, a series of polythermal sections and an isothermal section at room temperature of the phase diagram (Fig. 11). In this system, as in the sulfur-containing system, three ternary compounds $CuBi_3Se_5$, $CuBiSe_2$ and Cu_3BiSe_3 were identified. These compounds melt incongruently.

The Cu-Bi-Te system. According to available data [21], no ternary compounds are formed in this system.

Table 13 shows data on the standard integral thermodynamic functions of copper-antimony and medibismuth chalcogenides. For almost all of these compounds, complete sets of thermodynamic quantities were obtained using the EMF method with a Cu^+ conducting electrolyte. The thermodynamic functions of $CuBi_3Se_5$, $CuBiSe_2$ and Cu_3BiSe_3, determined by the EDS method [59, 221] (exception for the $-\Delta_f G^0(298K)$ of the last compound) are in good agreement with calorimetric data [223, 224].

Conclusion

This work summarizes the results of studies, including ours, on the thermodynamic properties of copper chalcogenides with heavy p^1-p^3 elements. It is shown that, there are mutually consistent sets of data on solid-phase equilibria and fundamental thermodynamic functions for copper chalcogenides with thallium and with elements of the germanium and arsenic subgroups. It is also noted that most of the existing works were carried out using various modifications of the equilibrium method of chemical thermodynamics - the EMF method. Considering the exceptional importance of phase diagrams in studies by this method, in addition to thermodynamic data, this work also presents data on solid-phase equilibria of the corresponding systems.

Our analysis also showed that the thermodynamic properties of copper chalcogenides with gallium, indium and silicon have been practically not studied, and the available data are contradictory.

In conclusion, we note that the capabilities of the thermodynamic approach are not fully

used in the development of complex functional materials, in particular copper-based chalcogenides; the empirical approach often prevails. We consider it important to develop thermodynamic research and wide application of their results in the design of new complex chalcogenide materials.

Acknowledgment

This work is supported by the Azerbaijan Science Foundation – Grant No AEF-MCG-2022-1(42)-12/10/4-M-10.

References

1. Physical-chemical properties of semiconductor substances. Reference-book. Ed. By Novoselova A.V. and Lazareva V.B. Moscow: Nauka publ., 1976, 339 p. (in Russian)
2. Abrikosov N.Kh., Bankina V.F., Poretskaya L.V., Shelimova L.E., Skudnova E.V. Semiconductor Chalcogenides and Their Base Alloys, Moscow: Nauka Publ., 1968 (in Russian)
3. Scheer R., Schock H.W., Chalcogenide Photovoltaics: Physics, Technologies, and Thin Film Devices, Wiley-VCH, 2011, 384 p.
4. Ahluwalia G.K. Applications of Chalcogenides, Springer, 2016. 10.1007/978-3-319-41190-3
5. Woodrow P. Chalcogenides: Advances in Research and Applications, Nova Science Publishers, 2018, 111p.
6. Alonso-Vante N. Chalcogenide Materials for Energy Conversion: Pathways to Oxygen and Hydrogen Reactions, Springer, 2018, 226 p. https://doi.org/10.1007/978-3-319-89612-0
7. Khan M.M. Chalcogenide-Based Nanomaterials as Photocatalysts, Elsevier: Amsterdam, The Netherlands, 2021, 376 p.
8. Moore J.E. The birth of topological insulators // Nature, 2010, V. 464, pp. 194-198. https://doi.org/10.1038/nature08916
9. Otrokov M.M., Klimovskikh I.I., Bentmann H., Estyunin D., Zeugner A., Aliev Z.S., Gass S., Wolter A.U.B., Koroleva A.V., Shikin A.M., Blanco-Rey M., Hoffmann M., Rusinov I.P., Vyazovskaya A.Yu, Eremeev S.V., Koroteev Yu.M., Kuznetsov V.M., Freyse F., Sánchez-Barriga J., Amiraslanov I.R., Babanly M.B., Mamedov N.T., Abdullayev N.A., Zverev V.N., Alfonsov A., Kataev V., Büchner B., Schwier E.F., Kumar S., Kimura A., Petaccia L., Di Santo G., Vidal R.C., Schatz S., Kissner K., Ünzelmann M., Min C.H., Moser S., Peixoto T.R.F., Reinert F., Ernst A., Echenique P.M., Isaeva A., Chulkov E.V. Prediction and observation of an antiferromagnetic topological insulator // Nature, 2019, V. 576, pp. 416-422. https://doi.org/10.1038/s41586-019-1840-9
10. Hagmann A.J. Chalcogenide topological insulators. In Chalcogenide From 3D to 2D and Beyond. Woodhead Publishing Series in Electronic and Optical Materials, 2020, pp. 305-337. https://doi.org/10.1016/B978-0-08-102687-8.00015-4
11. Flammini R., Colonna S., Hogan C., Mahatha S., Papagno M., Barla A., Sheverdyaeva P., Moras P., Aliev Z., Babanly M.B. Evidence of β-antimonene at the Sb/Bi_2Se_3 interface // Nanotechnology, 2018, V. 29, no. 6, pp. 065704. 10.1088/1361-6528/aaa2c4
12. Pacile D., Eremeev S.V., Caputo M., Pisarra M., De Luca O., Grimaldi I., Fujii J., Aliev Z.S., Babanly M.B., Vobornik I., Agostino R.G., Goldoni A., Chulkov E.V., Papagno M., Deep insight into the electronic structure of ternary topological insulators: A comparative study of $PbBi_4Te_7$ and $PbBi_6Te_{10}$ // Phys. Stat. Sol. (RRL), 2018, V. 12, no. 12, pp. 1800341-8. https://doi.org/10.1002/pssr.201800341
13. Shvets I.A., Klimovskikh I.I., Aliev Z.S., Babanly M.B., Sánchez-Barriga J., Krivenkov M., Shikin A.M., Chulkov E.V. Impact of stoichiometry and disorder on the electronic structure of the $PbBi_2Te_{4-x}Se_x$ topological insulator // Phys. Rev. B, 2017, V. 96, pp. 235124 -7.

DOI:https://doi.org/10.1103/PhysRevB.96.235124

14. Nurmamat M., Okamoto K., Zhu S., Menshchikova T. V., Rusinov I. P., Korostelev V.O., Miyamoto K., Okuda T., Miyashita T., Wang X., Ishida Y., Sumida K., Schwier E.F., Ye M., Aliev Z.S., Babanly M.B., Amiraslanov I.R., Chulkov E.V., Kokh K.A., Tereshchenko O., Shimada K., Shin S., Kimura A. Topologically non-trivial phase-change compound $GeSb_2Te_4$ // ACS Nano 2020, V. 14, no. 7, pp. 9059-9065. https://doi.org/10.1021/acsnano.0c04145
15. Garnica M., Otrokov M.M., Aguilar P.C., Klimovskikh I.I., Estyunin D., Aliev Z.S., Amiraslanov I.R., Abdullayev N.A., Zverev V.N., Babanly M.B., Mamedov N.T., Shikin A.M., Arnau A., Vázquez de Parga A.L., Chulkov E.V., Miranda R. Native point defects and their implications for the Dirac point gap at $MnBi_2Te_4$(0001) // npj Quantum Mater., 2022, V. 7, pp. 7. https://doi.org/10.1038/s41535-021-00414-6
16. Jahangirli Z.A., Alizade E.H., Aliev Z.S., Otrokov M.M., Ismayilova N.A., Mammadov S.N., Amiraslanov I.R., Mamedov N.T., Orudjev G.S., Babanly M.B., Shikin A.M., Chulkov E.V. Electronic structure and dielectric function of Mn-Bi-Te layered compounds // J. Vac. Sci. Technol. B, 2019, V. 37, pp. 062910. https://doi.org/10.1116/1.5122702
17. Eremeev S.V., Rusinov I.P., Koroteev Yu.M., Vyazovskaya A.Yu., Hoffmann M., Echenique P.M., Ernst A., Otrokov M.M., Chulkov E.V. Topological Magnetic Materials of the $(MnSb_2Te_4)\cdot(Sb_2Te_3)_n$ van der Waals Compounds Family // J. Phys. Chem. Lett. 2021, V.12, no. 17, pp. 4268-4277. https://doi.org/10.1021/acs.jpclett.1c00875
18. Tian W., Yu W., Shi J., Wang Y. The Property, Preparation and Application of Topological Insulators: A Review // Materials (Basel), 2017, V. 10, no. 7, pp. 814. DOI: 10.3390/ma10070814
19. Pesin D., Macdonald A.H. Spintronics and pseudospintronics in graphene and topological insulators // Nat. Mater., 2012, V. 11, pp. 409-416. doi: 10.1038/nmat3305.
20. Babanly M.B., Chulkov E.V., Aliev Z.S., Shevel'kov A.V., Amiraslanov I.R. Phase diagrams in materials science of topological insulators based on metal chalcogenides // Russ. J. Inorg. Chem., 2017, V. 62, no. 13, pp. 1703-1729. https://doi.org/10.1134/S0036023617130034
21. Babanly M.B., Yusibov Y.A., and Abishev V.T., Ternary Chalcogenides Based on Copper and Silver. Baku, BSU, 1993, 342 p. (in Russian)
22. Xing C., Lei Y., Liu M., Wu S., He W. Environment-friendly Cu-based thin film solar cells: materials, devices and charge carrier dynamics // Phys. Chem. Chem. Phys., 2021, V. 23, pp. 16469-16487. https://doi.org/10.1039/D1CP02067F
23. Fu H. Environmentally friendly and earth-abundant colloidal chalcogenide nanocrystals for photovoltaic applications // J. Mater. Chem. C, 2018, V. 6, pp. 414-445. https://doi.org/10.1039/C7TC04952H
24. Kumar M., Meena B., Subramanyam P., Suryakala D., Subrahmanyam C. Emerging Copper-based semiconducting materials for photocathodic applications in solar driven water splitting // Catalysts, 2022, V. 12, no. 10, pp. 1198. doi: 10.3390/catal12101198
25. Khairy M., Jiang P., Boulet P., Record M-C. Electron Density and Optoelectronic Properties of Copper Antimony Sulphur Ternary Compounds for Photovoltaic Applications. Journal of Electronic Materials, 2022, V.51, no.7, pp.3903-3918. https://doi.org/10.1007/s11664-022-09650-3
26. Amrillah T., Prasetio A., Supandi A., Sidiq D., Putra F., Nugroho M., Salsabilla Z., Azmi R. Environment-friendly copper-based chalcogenide thin film solar cells: status and perspectives // Mater. Horiz., 2023, V. 10, pp. 313-339. https://doi.org/10.1039/D2MH00983H
27. Palchoudhury S., Ramasamy K., Gupta A. Multinary copper-based chalcogenide nanocrystal systems from the perspective of device applications // Nanoscale Adv.,

2020, V. 2, no. 8, pp. 3069-3082. doi: 10.1039/d0na00399a.
28. Wei T.R., Qin Y., Deng T., Song Q., Jiang B., Liu R., Qiu P., Shi X., Chen L. Copper chalcogenide thermoelectric materials // Sci. China Mater., 2019, V. 62, pp. 8-24. doi: 10.1007/s40843-018-9314-5
29. Liu H., Shi X., Xu F., Zhang L., Zhang W., Chen L., Li Q., Uher C., Day T., Snyder G.J. Copper ion liquid-like thermoelectrics // Nature Mater., 2012, V. 11, no. 5, pp. 422-425. doi:10.1038/nmat3273
30. Viswanath A.K., Radhakrishna S. Copper Ion Conductors // High Conductivity Solid Ionic Conductors, 1989, pp. 280-326. doi:10.1142/9789814434294_0012
31. Nilges T., Pfitzner A. A structural differentiation of quaternary copper argyrodites: structure – property relations of high temperature ion conductors // Z. Kristallogr., 2005, V. 220, no. 2-3, pp. 281-294. https://doi.org/10.1524/zkri.220.2.281.59142
32. Gorin Y.F., Mel'nikova N.V., Baranova E.R., Kobeleva O.L. Influence of ionic conductivity on the elastic characteristics of four-component copper and silver chalcogenides // Tech. Phys. Lett., 1997, V. 23, pp. 550-552. https://doi.org/10.1134/1.1261873
33. Ivanov-Shchits A.K., Murin I.V. Solid State Ionics. Petersburg Univ., 2000, vol. 1, 616 p.
34. Wu X., Liu K., Wang R., Yang G., Lin J., Liu X. Multifunctional $CuBiS_2$ Nanoparticles for Computed Tomography Guided Photothermal Therapy in Preventing Arterial Restenosis After Endovascular Treatment // Front. Bioeng. Biotechnol., 2020, V. 8. https://doi.org/10.3389/fbioe.2020.585631
35. Askari N., Askari M.B. Apoptosis-inducing and image-guided photothermal properties of smart nano CuBiS2 // Mater. Res. Express 2019, V. 6, pp. 065404. doi: 10.1088/2053-1591/ab0c3e
36. Mindat.org: Open database of minerals, rocks, meteorites and the localities they come from. Available at http://www.mindat.org (accessed August 23, 2018)
37. Filippou D., Germain P., Grammatikopoulos T. Recovery Of Metal Values From Copper—Arsenic Minerals And Other Related Resources // Miner. Process. Extr. Metall. Rev., 2007, V. 28, pp. 247-298. https://doi.org/10.1080/08827500601013009
38. Babanly M.B., Mashadiyeva L.F., Babanly D.M., Imamaliyeva S.Z., Taghiyev D.B., Yusibov Y.A. Some issues of complex investigation of the phase equilibria and thermodynamic properties of the ternary chalcogenide systems by the EMF method // Russ. J. Inorg. Chem., 2019, V. 64, no. 13, pp. 1649-1671. https://doi.org/10.1134/S0036023619130035
39. West D.R.F. Ternary Phase Diagrams in Materials Science. Boca Raton: CRC Press, 2013, 3rd edition, pp. 240. https://doi.org/10.1201/9781003077213
40. Saka H. Introduction To Phase Diagrams In Materials Science And Engineering. London: World Scientific Publishing Company, 2020, pp.188. https://doi.org/10.1142/11368
41. Wagner K. Thermodynamics of alloys. M.: Metallurgizdat, 1957, 179 p.
42. Morachevsky A.G., Voronin G.F., Heiderich V.A., Kutsenok I.B. Electrochemical methods of research in the thermodynamics of metallic systems. ICC "Akademkniga", 2003, 334 pp.
43. Babanly M.B., Yusibov Yu.A. Electrochemical Methods in Thermodynamics of Inorganic Systems. Baku: ELM. 2011. 306 p. (in Russian)
44. Babanly M.B., Yusibov Yu.A., Abishev V.T. EMF method in the thermodynamics of complex semiconductor substances. Baku: BSU, 1992, 317 p.
45. Babanly M.B., Yusibov Yu.A., Babanly N.B. The EMF method with solid-state electrolyte in the thermodynamic investigation of ternary copper and silver chalcogenides. Electromotive force and measurement in several systems // Ed.S.Kara. Intechweb.

Org, 2011, pp. 57-78. DOI: 10.5772/28934
46. Babanly N.B., Orujlu E.N., S.Z.Imamaliyeva, Y.A.Yusibov, M.B.Babanly. Thermodynamic investigation of silver-thallium tellurides by EMF method with solid electrolyte Ag_4RbI_5 // J.Chem. Thermodyn., 2019, V.128, pp. 78-86. https://doi.org/10.1016/j.jct.2018.08.012
47. Imamaliyeva S.Z., Musayeva S.S., Babanly D.M., Jafarov Y.I., Tagiyev D.B., Babanly M.B. Determination of the thermodynamic functions of bismuth chalcoiodides by EMF method with morpholinium formate as electrolyte // Thermochim. Acta, 2019, V. 679, pp. 178319 https://doi.org/10.1016/j.tca.2019.178319
48. Aliev Z.S., Musayeva S.S., Imamaliyeva S.Z., Babanlı M.B. Thermodynamic study of antimony chalcoiodides by EMF method with an ionic liquid // J. Therm. Anal. Calorim., 2018, V. 133, no. 2, pp. 1115-1120. https://doi.org/10.1007/s10973-017-6812-4
49. Hasanova G.S., Aghazade A.I., Imamaliyeva S.Z., Yusibov Y.A., Babanly M.B. Refinement of the Phase Diagram of the Bi-Te System and the Thermodynamic Properties of Lower Bismuth Tellurides // JOM, 2021, V. 73, no. 5, pp. 1511-1521. https://doi.org/10.1007/s11837-021-04621-1
50. Babanly D.M., Velieva G.M., Imamaliyeva S.Z., Babanly M.B. Thermodynamic functions of arsenic selenides // Russ. J. Phys. Chem. A, 2017, V. 91, no. 7, pp. 1170-1173. https://doi.org/10.1134/S0036024417070044
51. Imamaliyeva S.Z., Babanly D.M., Gasanly T.M., Tagiyev D.B., Babanly M.B. Thermodynamic Properties of Tl_9GdTe_6 and $TlGdTe_2$ // Russ. J. Phys. Chem. A, 2018, V. 92, no. 11, pp. 2111-2117. https://doi.org/10.1134/S0036024418110158
52. Jafarov Y.I., Ismaylova S.A., Aliev Z.S., Imamaliyeva S.Z., Yusibov Y.A., Babanly M.B. Experimental study of the phase diagram and thermodynamic properties of the Tl-Sb-S system // CALPHAD, 2016, V. 55, pp. 231-237. https://doi.org/10.1016/j.calphad.2016.09.007
53. Alakbarova T.M., Orujlu E.N., Babanly D.M., Imamaliyeva S.Z., Babanly M.B. Solid-phase equilibria in the $GeBi_2Te_4$-Bi_2Te_3-Te system and thermodynamic properties of compounds of the $GeTe{\cdot}mBi_2Te_3$ homologous series // Phys. Chem. Solid State, 2022, V. 23, no. 1, p. 25-33. https://doi.org/10.15330/pcss.23.1.25-33
54. Babanly D.M., Huseynov G.M., Aliev Z.S., Taghiyev D.B., Babanlı M.B. Thermodynamic Study of Tl_6SBr_4 Compound and Some Regularities in Thermodynamic Properties of Thallium Chalcohalides // Adv. Mater. Sci. Eng., 2017, pp. 1-9. https://doi.org/10.1155/2017/5370289
55. Babanly M.B., Kulieva N.A. Phase diagram and thermodynamic properties of the Tl-Ge-Se system // Russ.J.Inorg. Chem., 1986, V. 31, no. 9, p. 2365-2371.
56. Kozin L.F., Nigmetova R.Sh., Dergacheva M.B. Thermodynamics of binary amalgam systems. Alma-Ata: Science, 1977, 343 p.
57. Bradley J.N., Greene P.D. Solids with High Ionic Conductivity in Group 1 Halide Systems // Trans. Faradey Soc., 1967, V. 63, no. 530, pt.II, pp. 424-430. DOI https://doi.org/10.1039/TF9676300424
58. Takahashi T., Yamamoto O., Yamada S., Hayashi S. Solid-State Ionics: High Copper Ion Conductivity of the System CuCl - CuI - RbCl // J. Electrochem. Soc., 1979, V. 126, no. 10, pp. 1654. DOI:10.1149/1.2128770
59. Babanly N.B., Yusibov Y.A., Mirzoyeva R.J., Shykhiyev Yu.M., Babanly M.B. $Cu_4RbCl_3I_2$ solid superionic conductor in thermodynamic study of three-component copper chalcogenides // Russ J Electrochem, 2009, V.45, pp. 405–410. https://doi.org/10.1134/S1023193509040089 .
60. Babanly M.B., Mashadieva L.F., Velieva G.M., Imamaliyeva S.Z., Shykhiyev Yu.M. Thermodynamic study of the Ag-As-Se and Ag-S-I systems using the EMF

method with a solid Ag_4RbI_5 electrolyte. // Russ J Electrochem, 2009, V.45, pp.399–404. https://doi.org/10.1134/S1023193509040077

61. Alverdiev I.D., Bagkheri S.M., Imamaliyeva S.Z., Yusibov Y.A., Babanly M.B. Thermodynamic study of Ag_8GeSe_6 by EMF with an Ag_4RbI_5 solid electrolyte // Russ J. Electrochem., 2017, V.53, no. 5, pp. 551-554. https://doi.org/10.1134/S1023193517050032
62. Babanly N.B., Imamaliyeva S.Z., Yusibov Y.A., Taghiyev D.B., Babanly M.B. Thermodynamic study of the Ag-Tl-Se system using the EMF method with Ag_4RbI_5 as a solid electrolyte // J. Solid State Electr., 2018, V. 22, pp. 1143-1148. https://doi.org/10.1007/s10008-017-3853-3
63. Alverdiev I.D., Imamalieva S.Z., Babanly D.M., Tagiev D.B., Babanly M.B. Thermodynamic Study of Silver—Tin Selenides by the EMF Method with Ag_4RbI_5 Solid Electrolyte // Russ. J. Electrochem., 2019, V. 55, no. 5, pp. 467-474. https://doi.org/10.1134/S1023193519050021
64. Moroz M., Tesfaye F., Demchenko P., Prokhorenko M., Kogut Yu., Pereviznyk O., Prokhorenko S., Reshetnyak O., Solid-state electrochemical synthesis and thermodynamic properties of selected compounds in the Ag–Fe–Pb–Se system // Solid State Sci., 2020, V. 107, pp. 106344(1-9). https://doi.org/10.1016/j.solidstatesciences.2020.106344
65. Moroz M., Tesfaye F., Demchenko P., Prokhorenko M., Yarema N., Lindberg D., Reshetnyak O., Hupa L. The equilibrium phase formation and thermodynamic properties of functional tellurides in the Ag–Fe–Ge–Te system // Energies, 2021, V. 14, no. 5, pp. 1314(1-15). https://doi.org/10.3390/en14051314
66. Moroz M., Tesfaye F., Demchenko P., Prokhorenko M., Prokhorenko S., Reshetnyak O. Non-activation synthesis and thermodynamic properties of ternary compounds of the Ag–Te–Br system // Thermochim. Acta, 2021, V. 698, pp. 178862(1–7). https://doi.org/10.1016/j.tca.2021.178862
67. Moroz M., Tesfaye F., Demchenko P., Prokhorenko M., Prokhorenko S., Reshetnyak O. Synthesis and thermodynamic investigation of energy materials in the Ag–Te–Cl system by the solid-state galvanic cells // JOM, 2021, V. 73, no. 5, pp. 1487-1494. https://doi.org/10.1007/s11837-021-04619-9
68. Bayramova U.R., Poladova A.N., Mashadiyeva L.F., Babanly M.B. Calorimetric determination of phase transitions of Ag_8BX_6 (B=Ge, Sn; X=S, Se) compounds // Condensed Matter and Interphases, 2022, V. 24, no. 2, pp. 187-195. https://doi.org/10.17308/kcmf.2022.24/9258
69. Bayramova U.R. Determination of the thermodynamic functions of the phase transition of the Cu_8SiSe_6 compound by the DSC method // Chem. Problems, 2022, no. 2, pp. 116-121.
70. Bayramova U.R., Babanly K.N., Ahmadov E.I., Mashadiyeva L.F., Babanly M.B. Phase equilibria in the Cu_2S-Cu_8SiS_6-Cu_8GeS_6 system and thermodynamic functions of phase transitions of the $Cu_8Si_{(1-X)}Ge_XS_6$ argyrodite phases // J. Equilib. Diff., 2023, V. 44, pp. 509-519. DOI: 10.1007/s11669-023-01054-y
71. Vijayan K., Thirumalaisamy L., Vijayachamundeeswari S.P., Sivaperuman K., Ahsan N., Okada Y. A Novel Approach for Designing a Sub-Bandgap in $CuGa(S,Te)_2$ Thin Films Assisted with Numerical Simulation of Solar Cell Devices for Photovoltaic Application // ACS Omega, 2023, V. 8, no. 25, pp. 22414-22427. https://doi.org/10.1021/acsomega.2c08196
72. Vijayan K., Vijayachamundeeswari S.P. Scrutinizing the effect of substrate temperature and enhancing the multifunctional attributes of spray

deposited copper gallium sulfide ($CuGaS_2$) thin films // Phase Transit., 2023, pp. 607-619. DOI:10.1080/01411594.2023.2238110

73. Maeda T., Nakanishi R., Yanagita M., Wada T. Control of electronic structure in Cu(In, Ga)(S, Se)$_2$ for high-efficiency solar cells // Jpn. J. Appl. Phys., 2020, V. 59, SGGF12. https://doi.org/10.35848/1347-4065/ab69e0
74. Shukla S., Sood M., Adeleye D., Peedle S., Kusch G., Dahliah D., Melchiorre M., Rignanese G.-M., Hautier G., Oliver R., Siebentritt S. Over 15% efficient wide-band-gap Cu(In,Ga)S_2 solar cell: Suppressing bulk and interface recombination through composition engineering // Joule, 2021, V. 5, no. 7, pp. 1816-1831. https://doi.org/10.1016/j.joule.2021.05.004
75. Levcenco S., Doka S., Tezlevan V., Marron D.F., Kulyuk L., Schedel-Niedrig T., Lux-Steiner M.Ch., Arushanov E. Temperature dependence of the exciton gap in monocrystalline $CuGaS_2$ // Physica B: Condensed Matter., 2010, V. 405, no. 17, pp. 3547-3550. https://doi.org/10.1016/j.physb.2010.05.037
76. Fan F.J., Liang Wu L., Yu S.-H. Energetic I-III-VI_2 and I_2-II-IV-VI_4 nanocrystals: synthesis, photovoltaic and thermoelectric applications **//** Energy Environ. Sci.**,** 2014, V. **7**, pp. 190-208. https://doi.org/10.1039/C3EE41437J
77. Yang Y., Xiong X., Han J. Modification of surface and interface of copper indium gallium selenide thin films with sulfurization // Emerg. Mater. Res., 2022, V. 11, no. 3, pp. 325-330. https://doi.org/10.1680/jemmr.21.00171
78. Stanbery B.J., Abou-Ras D., Yamada A., Mansfield L. CIGS photovoltaics: reviewing an evolving paradigm // J. Phys. D: Appl. Phys., 2021, V. 55, no. 17, pp. 173001. DOI 10.1088/1361-6463/ac4363
79. Li W., Song Q., Zhao C., Qi T., Zhang C., Wang W., Gao C., X., Ning D., Ma M., Zhang J., Feng Y., Chen M., Li W., Yang C. Toward High-Efficiency Cu(In,Ga)(S,Se)$_2$ Solar Cells by a Simultaneous Selenization and Sulfurization Rapid Thermal Process // ACS Appl. Energy Mater., 2021, V. 4, no. 12, pp. 14546-14553. https://doi.org/10.1021/acsaem.1c03198
80. Khavari F., Keller J., Larsen J.K., Sopiha K.V., Törndahl T., Edoff M. Comparison of Sulfur Incorporation into $CuInSe_2$ and $CuGaSe_2$ Thin-Film Solar Absorbers // Phys. Status Solidi A, 2020, V. 217, no. 22. https://doi.org/10.1002/pssa.202000415
81. Nakamura M., Yamaguchi K., Kimoto Y., Yasaki Y., Kato T., Sugimoto H. Cd-free Cu(In,Ga)(Se,S)$_2$ thin-film solar cell with record efficiency of 23.35% // IEEE J. Photovolt., 2019, V. 9, no. 6, pp. 1863-1867. doi: 10.1109/JPHOTOV.2019.2937218
82. Hollingsworth J.A., Banger K.K., Jin M.H.C., Harris J.D., Cowen J.E., Bohannan E.W., Switzer J.A, Buhro W.E., Hepp A.F. Single source precursors for fabrication of I-III-VI_2 thin-film solar cells via spray CVD // Thin Solid Films , 2003, V. 431-432, pp. 63-67. https://doi.org/10.1016/S0040-6090(03)00196-2
83. Kim J.-H., Han H., Kim M.K., Ahn J., Hwang D.K., Shin T.J., Min B.K., Lim J.A. Solution-processed near-infrared Cu(In,Ga)(S,Se)$_2$ photodetectors with enhanced chalcopyrite crystallization and bandgap grading structure via potassium incorporation // Sci Rep. 2021, V. 11, pp. 7820. doi: 10.1038/s41598-021-87359-9
84. Clarke D., Breguel R. Analysis of Thermodynamic Properties of Cu(In,Ga)Se_2 Thin-Film Solar Cells for Viable Space Application // PAM Review: Energy Science & Technology, 2018, V. 5, pp. 131-149. http://dx.doi.org/10.5130/pamr.v5i0.1501
85. Torimoto T., Kameyama T., Uematsu T., Kuwabata S. Controlling optical properties and electronic energy structure of I–III–VI semiconductor quantum dots for improving their photofunctions // J. Photochem. Photobiol., C, 2023, V. 54, pp. 100569. https://doi.org/10.1016/j.jphotochemrev.2022.100569
86. Gullu H.H., Isik M., Gasanly N.M. Structural and optical properties of

thermally evaporated Cu-Ga-S (CGS) thin films // Physica B: Condensed Matter., 2018, V. 547, pp. 92-96. https://doi.org/10.1016/j.physb.2018.08.015
87. Soni A., Gupta V., Arora C.M., Dashora A., Ahuja B.L. Electronic structure and optical properties of $CuGaS_2$ and $CuInS_2$ solar cell materials // Solar Energy, 2010, V. 84, no. 8, pp. 1481-1489. https://doi.org/10.1016/j.solener.2010.05.010
88. Candeias M.B., Fernandes T.V., Falcão B.P. , Cunha A.F., Cunha J.M.V., Barbosa J., Teixeira J.P., Fernandes P.A., Peres M., Lorenz K., Salomé P.M.P., Leitão J.P. Cu(In,Ga)Se_2-based solar cells for space applications: proton irradiation and annealing recovery // J. Mater. Sci., 2023, V. 58, pp. 16385-16401. https://doi.org/10.1007/s10853-023-09033-x
89. Jiang C., Tozawa M., Akiyoshi K., Kameyama T., Yamamoto T., Motomura G., Fujisaki Y., Uematsu T., Kuwabata S., Torimoto T. Development of Cu–In–Ga–S quantum dots with a narrow emission peak for red electroluminescence // *J. Chem. Phys., 2023, V.* 158, pp. 164708. https://doi.org/10.1063/5.0144271
90. Kim Y.-K., Ahn S.-H., Chung K., Cho Y.-S., Choi C.-J. The photoluminescence of $CuInS_2$ nanocrystals: Effect of non-stoichiometry and surface modification // J. Mater. Chem., 2012, V. 22, pp. 1516-1520. https://doi.org/10.1039/c1jm13170b
91. Isik M., Gasanly N.M., Gasanova L.G., Mahammadov A.Z. Thermoluminescence study in $Cu_3Ga_5S_9$ single crystals: application of heating rate and T_m-T_{stop} methods // J. Lumin., 2018, V. 199, pp. 334-338. https://doi.org/10.1016/j.jlumin.2018.03.076
92. Porras G.P.S., Wasim S.M. Thermal properties of p-type $CuInSe_2$ // Phys. Status Solidi A, 1980, V. 59, no. 2, pp. K175-K178. https://doi.org/10.1002/pssa.2210590268
93. Rincón C., Valeri-Gil M.L., Wasim S.M. Room-Temperature Thermal Conductivity and Grüneisen Parameter of the I–III–VI_2 Chalcopyrite Compounds // Phys. Status Solidi A, 2006, V. 147, no. 2, pp. 409-415. https://doi.org/10.1002/pssa.2211470212
94. Kurosaki K., Goto K., Kosuga A., Yamanaka S. Thermoelectric and Thermophysical Characteristics of Cu_2Te-Tl_2Te Pseudo Binary System // Mater. Trans., 2006, V. 47, no. 6, pp. 1432-1435. https://doi.org/10.2320/matertrans.47.1432
95. Matsumoto H., Kurosaki K., Muta H., Yamanaka S. Thermoelectric Properties of $TlCu_3Te_2$ and $TlCu_2Te_2$ // J. Electron. Mater., 2009, V. 38, pp. 1350-1353. https://doi.org/10.1007/s11664-009-0664-z
96. Ueno T., Nagasaki K., Horikawa T., Kawakami M., Kondo K. Phase equilibria in the system Cu–Ga–S at 500° and 400°C // The Canadian Mineralogist, 2005, V. 43, no. 5, pp. 1653-1661. https://doi.org/10.2113/gscanmin.43.5.1653
97. Mikkelsen J.C. Ternary phase relations of the chalcopyrite compound $CuGaSe_2$ // J. Electron. Mater., 1981, V. 10, no. 3, pp. 541-558. https://doi.org/10.1007/BF02654590
98. Wu H.-J., Dong Z.-J. Phase diagram of ternary Cu-Ga-Te system and thermoelectric properties of chalcopyrite $CuGaTe_2$ materials // Acta Mater., 2016, V. 118, pp. 331-341. https://doi.org/10.1016/j.actamat.2016.07.060
99. *Migge H. Thermochemistry in the system Cu–In–S at 298 K // J. Mater. Res., V. 6, no. 11, pp. 2381-2386.* DOI: https://doi.org/10.1557/JMR.1991.2381
100. Wiedemeier H., Santandrea R. Mass spectrometric studies of the Decomposition and the Heat of Formation of $CuInS_2$(s) // Z. anorg. allg. Chem., 1983, V. 497, no. 2, pp. 105-118. https://doi.org/10.1002/zaac.19834970210
101. Neumann H. Nonstoichiometry and electrical properties of $CuGaSe_2$ and $AgInTe_2$ // Cryst. Res. Technol., 1983, V. 18, no. 1, pp. K8–K11. https://doi.org/10.1002/crat.2170180123

102. Jianyun S., Kim W.K., Shunli S., Maoyou C., Song C., Anderson T.J. Thermodynamic description of the ternary compounds in the Cu-In-Se system // Rare Metals, 2006, V. 25, no. 5, pp. 481-487. https://doi.org/10.1016/S1001-0521(06)60088-0
103. Abishev V.T., Babanly M.B., Kuliyev A.A. Phase equilibria in the Tl_2S–Cu_2S system // Izv.VUZov. ser. Chem. and Chem. Thecnol., 1978, V. 21, no. 5, pp. 630-632.
104. Mammadov M.I., Alizade M.Z., Zamanov S.K., Aliyev O.M. Study of the phase diagram of the Tl_2S-Cu_2S system // Russ. J. Inorg. Chem., 1978, V. 14, no. 8, pp. 1527-1529.
105. Sobbott E. Das System Tl_2S-Cu_2S // Monatsh. Chem. B, 1994, V.115, no. 12, pp. 1397-1400. https://doi.org/10.1007/BF00816337
106. Babanly M.B., Un L.T., Kuliev A.A. System Tl–Tl_2S–CuTlS–Cu // Russ. J. Inorg. Chem., 1985, V. 30, no. 4, p. 1043-1046
107. Babanly M.B., Un L.T., Kuliev A.A. System Tl_2S–CuTlS–S // Russ. J. Inorg. Chem., 1985, V. 30, no. 4, p. 1047-1050
108. Babanly M.B., Un L.T., Kuliev A.A. System Cu-Tl-S // Russ. J. Inorg. Chem., 1986, V. 32, no.7, p. 1837-1844.
109. Babanly N.B., Aliev Z.S., Yusibov Yu.A., Babanly M.B. A thermodynamic study of Cu—Tl—S system by EMF method with $Cu_4RbCl_3I_2$ solid electrolyte. Russ J Electrochem 46, 354–358 (2010). https://doi.org/10.1134/S1023193510030146 .
110. Vasiliev V.P., Nikolskaya A.V., Chernyshev V.V., Gerasimov Ya.I. Thermodynamic properties of thallium sulfides // Proceedings of the USSR Academy of Sciences. Inorganic materials, 1973, V. 9, no. 6, p. 900-903.
111. Azizov T.Kh., Aliev I.Ya., Mustafaev F.M., Abbasov A.S. Thermodynamic properties of copper chalcogenides / In the book. Thermodynamic properties of hard metal alloys. Minsk: BSU, 1976, p. 86-87.
112. Kubaschewski O., Alcock C.B., Spenser P.J. Materials Thermochemistry. Pergamon Press, 1993, 350 p.
113. Abishov V.T., Babanly M.B., Kuliev A.A. Phase equilibria in the Cu_2Se-Tl_2Se system // Inorg. Materials, 1979, V. 15, no. 11, p. 1926.
114. Voroshilov Yu.V., Evstigneeva T.L., Nekrasov I.Ya. Crystal chemical tables of ternary chalcogenides. M.: Nauka, 1989, 224 p.
115. Babanly N.B. Thermodynamic properties of some ternary phases of the Cu-Tl-Se system // Inorg Mater, 2011, V.47, pp. 1306–1310. https://doi.org/10.1134/S0020168511120016
116. Kleep K.O. Darstellung und Kristallostructur von $TlCu_3Te_2$: ein Tellurocuprat mit aufgefuelltem $CuAl_2$-typ // J. Less-Common Metals, 1987, V. 127, pp. 79-89.
117. Bradtmöller S., Böttcher P. Crystal structure of copper tetrathallium trutelluride $CuTl_4Te_3$ // Z. Kristallogr., 1994, V. 209, pp. 97.
118. Babanly N.B., Salimov Z.E., Akhmedov M.M., Babanly M.B. Thermodynamic study of the Cu–Tl–Te system by the EMF method with solid electrolyte $Cu_4RbCl_3I_2$ // Russ. J. Electrochem, 2012, V.48, pp.68–73. https://doi.org/10.1134/S1023193512010041
119. Babanly, M.B., Salimov, Z.E., Babanly, N.B., Imamaliyeva S.Z. Thermodynamic properties of copper thallium tellurides. // Inorg Mater, 2011, V.47, pp.361–364. https://doi.org/10.1134/S0020168511040030
120. Cheng, X., Li Z., You Y., Zhu T., Yan Y., Su X., Tang X. Role of Cation Vacancies in Cu_2SnSe_3 Thermoelectrics // ACS Appl. Mater. Interfaces, 2019, V. 11, pp. 24212-24220. https://doi.org/10.1021/acsami.9b01348
121. Hung T., Yan Y., Peng K., Tang X., Guo L., Wang R., Lu X., Zhou X., Wang G. Enhanced thermoelectric performance in copper-deficient Cu_2GeSe_3 // J. Alloys Compd., 2017, V. 723, pp. 708-713. https://doi.org/10.1016/j.jallcom.2017.06.133

122. Jacob S., Delatouche B., Péré D., Jacob A., Chmielowski R. Insights into the thermoelectric properties of the $Cu_2Ge(S_{1-x}Se_x)_3$ solid solutions // Mater. Today, 2017, V. 4, pp. 12349-12359. https://doi.org/10.1016/j.matpr.2017.10.003
123. Li Y., Cao T., Liu G., Liu L.M., Li J., Chen K., Li L., Han Y., Zhou M. Enhanced Thermoelectric Properties of Cu_2SnSe_3 by (Ag, In)-Co-Doping // Adv. Funct. Mater., 2016, V. 26, pp. 6025-6032. https://doi.org/10.1002/adfm.201601486
124. Ma R.L., Liu G., Li Y., Li J., Chen K., Han Y., Zhou M., Li L. Thermo-electric properties of S and Te-doped Cu_2SnSe_3 prepared by combustion synthesis // J. Asian Ceram. Soc., 2018, pp.13-19. DOI: 10.1080/21870764.2018.1439609
125. Ma R.L., Liu G., Li J., Li Y., Chen K., Han Y., Zhou M., Li L. Effect of secondary phases on thermoelectric properties of Cu_2SnSe_3 // Ceram. Int., 2017, V. 43, no. 9, pp. 7002-7010. https://doi.org/10.1016/j.ceramint.2017.02.126
126. Prasad S, Rao A., Gahtori B., Bathula S., Dhar A., Du J.-S., Kuo Y.-K. The low and high temperature thermoelectric properties of Sb doped Cu_2SnSe_3 // Mater. Res. Bull., 2016, V. 83, pp. 160-166. https://doi.org/10.1016/j.materresbull.2016.06.002
127. Prasadh D., Sarkar B., Arulgnanam A. First-principles study on the electrical properties of Cu_2GeSe_3 compound // MMSE Journal, 2018, V. 14, no. 1, pp. 1-5. 10.2412/mmse.98.61.409.
128. Siyar, M., Siyar M., Cho J.Y., Jin W.C., Hwang E.U., Kim M., Parker C. Thermoelectric Properties of Cu_2SnSe_3-SnS // J. Compos. Mater., 2019, V. 12, no. 13, pp. 2040-2043. doi: 10.3390/ma12132040
129. Wang R., Li A., Huang T., Zhang B., Peng K., Yang H., Lu X., Zhou X., Han X., Wang G. Enhanced thermoelectric performance in Cu_2GeSe_3 via (Ag, Ga)-co-doping on cation sites // J. Alloys Compd., 2018, V. 769, pp. 218-225. https://doi.org/10.1016/j.jallcom.2018.07.318
130. Zhao D., Wang X., Wu D. Enhanced Thermoelectric Properties of Graphene, Cu_2SnSe_3 Composites // Crystals, 2017, V. 7, pp. 71. https://doi.org/10.3390/cryst7030071
131. Reinders A., Verlinden P., Sark W. Photovoltaic Solar Energy: From Fundamentals to Applications. 2017, 718 p.
132. Bayazıt T., Olgar M.A., Küçükömeroğlu T., Bacaksız E., Tomakin M. Growth and characterization of Cu_2SnS_3 (CTS), Cu_2SnSe_3 (CTSe), and $Cu_2Sn(S,Se)_3$ (CTSSe) thin lms using dip-coated Cu–Sn precursor // J. Mater. Sci.: Mater. Electron., 2019, V. 13, p. 1-7. https://doi.org/10.1007/s10854-019-01622-4
133. Matthews P.D., McNaughter P.D., Lewis D.J., Brien P. Shining a light on transition metal chalcogenides for sustainable photovoltaics // Chem. Sci., 2017, V. 8, no. 6, pp. 4177-4187. https://doi.org/10.1039/C7SC00642J
134. Pejjai B., Reddy V.R.M., Gedi S., Park C. Review on earth-abundant and environmentally benign Cu–Sn–X(X = S, Se) nanoparticles by chemical synthesis for sustainable solar energy conversion // J. Ind. Eng. Chem., 2018, V. 60, pp. 19-52. https://doi.org/10.1016/j.jiec.2017.09.033
135. Shigemi A., Wada T. First-principles studies on the interface between light-absorbing layer and Mo back electrode in $Cu(In, Ga)Se_2$, $Cu_2ZnSn(S, Se)_4$, and Cu_2SnS_3 solar cells // Jpn. J. Appl. Phys., *2018*, *V.* 57, pp. 08RC17. DOI 10.7567/JJAP.57.08RC17
136. Chantana J., Chantana J., Uegaki H., Minemoto T. Influence of Na in Cu_2SnS_3 film on its physical properties and photovoltaic performances // Thin Solid Films, 2017, V. 636, pp. 431-437. https://doi.org/10.1016/j.tsf.2017.06.044
137. Chaudhari J.J., Joshi U.S. Fabrication of high quality Cu_2SnS_3 thin film solar cell with 1.12% power conversion efficiency

obtain by low cost environment friendly sol-gel technique // Mater. Res. Express, 2018, V. 5, pp. 036203. 10.1088/2053-1591/aab20e
138. Chierchia R., Pigna F., Valentini M. Cu_2SnS_3 based solar cell with 3% efficiency // Phys. Status Solidi C, 2016, pp. 35-39. 10.1002/pssc.201510115
139. De Wild J., Babbe F., Robert E.V.C. Silver-Doped Cu_2SnS_3 Absorber Layers for Solar Cells Application // IEEE Journal of Photovoltaics, 2018, V. 8, pp. 299-304. 10.1109/JPHOTOV.2017.2764496
140. Oliva F., Arqués L., Acebo L. Characterization of Cu_2SnS_3 polymorphism and its impact on optoelectronic properties // J. Mater. Chem. A, 2017, V. 5, pp. 23863-23871. https://doi.org/10.1039/C7TA08705E
141. Reddy G.P., Reddy K.T.R. Preparation and Characterization of Cu_2SnS_3 Thin Films by Two Stage Process for Solar Cell Application // Mater. Today: Proc., 2017, V. 4, p. 12401-12406. https://doi.org/10.1016/j.matpr.2017.10.010
142. Shadrokh Z., Yazdani A., Eshghi A. Preparation and characterization of sphere-like Cu_2SnS_3 nanoparticles and their dropcasted thin films // *J. Semicond.*, *2017*, *V.* 38, pp. 013001. 10.1088/1674-4926/38/1/013001
143. Shelke H.D., Lokhande A.C., Lokhande C.D. Cu_2SnS_3 thin film: Structural, morphological, optical and photoelectrochemical studies // Surfaces and Interfaces, 2017, V. 9, pp. 23-27. https://doi.org/10.1016/j.surfin.2017.08.006
144. Lokhande A.C., Chalapathy R.B.V., He M., Joo E. Development of Cu_2SnS_3 (CTS) thin film solar cells by physical techniques: A status review // Solar Energy Materials and Solar cells, 2016, V. 153, p. 4-107. https://doi.org/10.1016/j.solmat.2016.04.003
145. Babanly M.B., Yusibov Y. A., Imamaliyeva S.Z. Babanly D.M., Alverdiyev I.J. al. Phase Diagrams in the Development of the Argyrodite Family Compounds and Solid Solutions Based on Them. J. Phase Equilib. Diffus. 2024. https://doi.org/10.1007/s11669-024-01088-w
146. Riess I, Mixed ionic–electronic conductors-material properties and applications // Solid State Ion., 2003, V. 157 no. 1-4, pp. 1-17. https://doi.org/10.1016/S0167-2738(02)00182-0
147. Yang C., Luo Y., Xia Y., Fang T., Du Z., Li X., Cui J. Improved Thermoelectric Performance of p-Type Argyrodite Cu_8GeSe_6 via the Simultaneous Engineering of the Electronic and Phonon Transports // ACS Appl. Mater. Interfaces, 2022, V. 14, pp. 16330-16337. https://doi.org/10.1021/acsami.2c02625
148. Zong P., Li Y., Negishi R., Li Z., Zhang C., Wan C. Thermoelectric Performance of Cu_8SiS_6 with High Electronic Band Degeneracy // ACS Appl. Electron. Mater., 2023. https://doi.org/10.1021/acsaelm.3c00423
149. Schwarzmüller S., Souchay D., Günther D., Gocke A., Dovgaliuk I., Miller S.A., Snyder G.J., Oeckler O. Argyrodite-Type $Cu_8GeSe_{6-x}Te_x$ ($0 \le x \le 2$): Temperature-Dependent Crystal Structure and Thermoelectric Properties // Z. Anorg. Allg. Chem., 2018, V. 664, pp. 1915-1922. https://doi.org/10.1002/zaac.201800453
150. Fan Y., Wang G., Wang R., Zhang B., Shen X., Jiang P., Zhang X., Gu H.-S., Lu X., Zhou X.-Y. Enhanced thermoelectric properties of p-type argyrodites Cu_8GeS_6 through Cu vacancy // J. Alloys Compd., 2020, V. 822, pp. 153665. https://doi.org/10.1016/j.jallcom.2020.153665
151. Jiang B., Qiu P., Eikeland E., Chen H., Song Q., Ren D., Zhang T., Yang J., Iversen B.B., Shi X., Chen L. Cu_8GeSe_6-based thermoelectric materials with an argyrodite structure // J. Mater. Chem. C, 2017, V. 5, pp. 943-952. https://doi.org/10.1039/C6TC05068A
152. Gao L., Lee M.-H., Zhang J. Metal-cation substitutions induced the enhancement of

second harmonic generation in A_8BS_6 (A = Cu, and Ag; B = Si, Ge, and Sn) // New J. Chem., 2019, V. 43, pp. 3719-3724. https://doi.org/10.1039/C8NJ06270F

153. Brammertz G., Vermang B., ElAnzeery H., Sahayaraj S., Ranjbar S., Meuris M., Poortmans J. Fabrication and characterization of ternary Cu_8SiS_6 and Cu_8SiSe_6 thin film layers for optoelectronic applications // Thin Solid Films, 2016, V. 616, pp. 649-654. https://doi.org/10.1016/j.tsf.2016.09.049
154. Olekseyuk I.D., Piskach L.V., Zhbankov O.Y., Parasyuk O.V., Kogut Y.M. Phase diagrams of the quasi-binary systems $Cu_2S–SiS_2$ and $Cu_2SiS_3–PbS$ and the crystal structure of the new quaternary compound Cu_2PbSiS_4 // J. Alloys Compd., 2005, V. 399, no. 1-2, pp. 149-154. https://doi.org/10.1016/j.jallcom.2005.03.086
155. Shpak O., Kogut Y., Fedorchuk A., Piskach L., Parasyuk O. The $Cu_2Se–PbSe–SiSe_2$ System and the Crystal Structure of $CuPb_{1,5}SiSe_4$ // *Lesia Ukrainka* Eastern *European National University Scientific Bulletin.* Inorg. and Phys.Chem. ser., 2014, 21(298), p 39-47.
156. Khanafer M., Rivet J., Flahaut J. Etude du système Cu_2S-GeS_2, Surstructure du composé Cu_2GeS_3. Transition de phase de Cu_8GeS_6 // Bull. Soc. chim. Fr., 1973, V. 3, pp. 859-862, (in French).
157. Alverdiyev I.J. Refinement of the phase diagram of the Cu_2S-GeS_2 system // Chem. Prob., 2019, V. 3, pp. 423-428. http://dx.doi.org/10.32737/2221-8688-2019-3-423-428
158. Carcaly C., Chezeau N., Rivet J., Flahaut J. Description of the systeme $GeSe_2$-Cu_2Se. Transition de phases du composé Cu_8GeSe_6 // Bull. Soc. chim. Fr., 1973, V. 1, no. 4, pp. 1191-1195, in French.
159. Rogacheva E.I., Melikhova N., Panasenko N.M. A Study of the System Cu_2Se-$GeSe_2$ // Inorg. Mater., 1975, V. 11, no. 5, pp. 719-722.
160. Piskach L.V., Parasyuk O.V., Romanyuk Ya.E. The phase equilibria in the quasi-binary $Cu_2GeS_3/Se_3/–CdS/Se/$ systems // J. Alloys Comp., 2000, V. 299, pp. 227-231. https://doi.org/10.1016/S0925-8388(99)00797-5
161. Alverdiyev I.J., Imamaliyeva S.Z., Akhmedov E.I., Yusibov Yu.A., Babanly M.B. Thermodynamic properties of some ternary compounds of the argyrodite family // Azerb. Chem. J., 2023, no. 4, pp. 21-30. doi.org/10.32737/0005-2531-2023-4-21-30
162. Yusibov Yu.A., Aliyeva Z.M., Babanly M.B. Thermodynamic properties of the Cu_2GeSe_3 compound // Azerb. Chem.J., 2023, no. 1, pp. 108-114. doi.org/10.32737/0005-2531-2023-1-108-114
163. Abbasov A.S., Aliyeva N.A., Aliyev I.Ya., Asadov Y.G., Askerova A.A. Thermodynamic properties of the Cu_2GeSe_3 and Cu_8GeSe_6 // Dokl. Akad. Nauk. Azerb. SSR., 1987, V. 42, no. 12, pp. 27-28.
164. Bayramova U.R., Ahmadov E.I., Babanly D.M., Mashadiyeva L.F., Babanly M.B. Calorimetric study of phase transition of Cu_8GeSe_6 and comparison with other argyrodite family compounds // Chem. Probl, 2023, no. 4 (21), pp. 396-403. DOI: 10.32737/2221-8688-2023-4-396-403
165. Mustafayev F.M., Abbasov A.S., Aliyev I.Ya. Thermodynamic investigation of the Cu_2S-SnS_2 // Dokl. AN Az. SSR., 1987, V. 43, no. 1, pp. 51-54 (In Russian)
166. Alverdiyev I.J. Thermodynamic study of Cu_2SnSe_3 by EMF method with solid electrolyte Cu_4RbCl_3I // AJP Fizika, 2019, V. XXV, no. 3, pp. 29-33.
167. Alverdiev I.J., Abbasova V.A., Yusibov Yu.A., Tagiev D.B., Babanly M.B. Thermodynamic Study of Cu_2GeS_3 and $Cu_{2-x}Ag_xGeS_3$ Solid Solutions by the EMF Method with a $Cu_4RbCl_3I_2$ Solid Electrolyte // Russ. J. Electrochem., 2018, V. 54, no. 2, pp. 153–158. DOI:10.5772/28934
168. Abbasova V.A., Alverdiyev I.J., Rahimoglu E., Mirzoyeva R.J., Babanly M.B. Phase relations in the Cu_8GeS_6-Ag_8GeS_6 system and some properties of solid solutions // Azerb. Chem. J., 2017, no.2, pp 25-29.

169. Mashadieva L.F., Alieva Z.M., Mirzoeva R.Dzh., Yusibov Yu.A., Shevel'kov A.V., Babanly M.B. Phase Equilibria in the $Cu_2Se–GeSe_2–SnSe_2$ System // Russ. J. Inorg. Chem., 2022, V. 67, no. 5, pp. 670-682. https://doi.org/10.1134/S0036023622050126
170. Bairamova U.R., Babanly K.N., Mashadieva L.F., Yusibov Yu.A., Babanly M.B. Phase Equilibria in the $Cu_2Se–Cu_8SiSe_6–Cu_8GeSe_6$ System // Russ. J. Inorg. Chem., 2023, no. 68, pp. 1611-1621. https://doi.org/10.1134/S0036023623602027
171. Bagheri S.M., Alverdiyev I.J., Aliev Z.S., Yusibov Y.A., Babanly M.B. Phase relationships in the $1.5GeS_2+Cu_2GeSe_3↔1.5GeSe_2+Cu_2GeS_3$ reciprocal system // J. Alloys Compd., 2015, V. 625, pp. 131-137. https://doi.org/10.1016/j.jallcom.2014.11.118
172. Alverdiyev I.J., Aliev Z.S., Bagheri S.M., Mashadiyeva L.F., Yusibov Y.A., Babanly M.B. Study of the $2Cu_2S+GeSe_2 ↔Cu_2Se+GeS_2$ reciprocal system and thermodynamic properties of the $Cu_8GeS_{6-x}Se_x$ solid solutions // J. Alloys Compd., 2017, v.691, pp.255-262. https://doi.org/10.1016/j.jallcom.2016.08.251
173. Alverdiev I.J., Abbasova V.A., Yusibov Yu.A., Babanly M.B. Thermodynamic properties of the Cu_8GeS_6-Ag_8GeS_6 solid solutions // Condensed Matter and Interphases, 2017, V. 19, no. 1, p. 22-26. https://doi.org/10.17308/kcmf.2017.19/172
174. Alverdiev I.J., Bagheri S.M., Aliyeva Z.M., Yusibov Yu.A., Babanly M.B. Phase Equilibria in the $Ag_2Se–GeSe_2–SnSe_2$ System and Thermodynamic Properties of $Ag_8Ge_{1–x}Sn_xSe_6$ Solid Solutions // Inorg. Mater., 2017, V. 53, no. 8, pp. 786-796. https://doi.org/10.1134/S0020168517080027
175. Mashadiyeva L.F., Kevser J.O., Aliev I.I., Yusibov Y.A., Tagiyev D.B., Aliev Z.S. The Ag_2Te-SnTe-Bi_2Te_3 system and thermodynamic properties of the $(2SnTe)_{1-x}(AgBiTe_2)_x$ solid solutions series //J. Alloys Compd., 2018, V. 724, pp.641-648. https://doi.org/10.1016/j.jallcom.2017.06.338
176. Centeno P., Alexandre M., Neves F., Fortunato E., Martins R., Águas H., Mendes M.J. Copper-Arsenic-Sulfide Thin-Films from Local Raw Materials Deposited via RF Co-Sputtering for Photovoltaics // *Nanomater.*, 2022, V. 12, no. 19, pp. 3268. https://doi.org/10.3390/nano12193268
177. McClary S.A., Taheri M.M., Blach D.D., Pradhan A.A., Li S., Huang L., Baxter C.B., Agrawal R. Nanosecond carrier lifetimes in solution-processed enargite (Cu_3AsS_4) thin films // Appl. Phys. Lett., 2020, V. 117, no. 16, pp. 162102. https://doi.org/10.1063/5.0023246
178. Studenyak I.P, Molnar Z.R., Makauz I.I. Deposition and optical absorption studies of Cu–As–S thin films // SPQEO, 2018, V.21, no.2, p. 167-172. https://doi.org/10.15407/spqeo21.02.167
179. Wallace S.K., Svane K.L., Huhn W.P., Zhu T., Mitzi D.B., Blum V., Walsh A. Candidate photoferroic absorber materials for thin-film solar cells from naturally occurring minerals: enargite, stephanite, and bournonite // Sustainable Energy & Fuels, 2017, V. 1, no. 6, pp. 1339-1350. https://doi.org/10.1039/C7SE00277G
180. Wallace S.K., Butler K.T., Hinuma Y., Walsh A. Finding a junction partner for candidate solar cell absorbers enargite and bournonite from electronic band and lattice matching // J. Appl. Phys, 2019, V. 125, pp. 055703. https://doi.org/10.1063/1.5079485
181. Ballow R.B., Miskin K.K., Abu-Omar M.M. Synthesis and Characterization of $Cu_3(Sb_{1–x}As_x)S_4$ Semiconducting Nanocrystal Alloys with Tunable Properties for Optoelectronic Device Applications // Chem. Mater., 2017, V. *29*, no. 2, pp. 573-578.

https://doi.org/10.1021/acs.chemmater.6b03850
182. Alqahtani T., Khan M.D., Lewis D.J., Zhong X.L., O'Brien P. Scalable synthesis of Cu–Sb–S phases from reactive melts of metal xanthates and effect of cationic manipulation on structural and optical properties // Sci. Rep., 2021, V. 11, no. 1, pp. 1-17. doi:10.1038/s41598-020-80951-5
183. Loranca-Ramos F.E., Diliegros-Godines C.J., Silva González R., Pal M. Structural, optical and electrical properties of copper antimony sulfide thin films grown by a citrate-assisted single chemical bath deposition // Appl. Surf. Sci., 2018, V. 427, pp. 1099-1106. doi:10.1016/j.apsusc.2017.08.02
184. Ornelas-Acosta R.E., Shaji S., Avellaneda D., Castillo G.A., Das Roy T.K., Krishnan B. Thin films of copper antimony sulfide: A photovoltaic absorber material // Mater. Res. Bull., 2015, V. 61, pp. 215-225. doi:10.1016/j.materresbull.2014.10.027
185. Vinayakumar V., Shaji S., Avellaneda D., Aguilar-Martínez J. A.and Krishnan B. Copper antimony sulfide thin films for visible to near infrared photodetector applications // *RSC Adv.***,** 2018, 8, 31055-31065. https://doi.org/10.1039/C8RA05662E
186. Van Embden J., Mendes J.O., Jasieniak J.J., Chesman A.S.R., Della Gaspera E. Solution-Processed $CuSbS_2$ Thin Films and Superstrate Solar Cells with CdS/In_2S_3 Buffer Layers // ACS Appl. Energy Mater., 2020, V. 3, no. 8, pp. 7885-7895. doi:10.1021/acsaem.0c01296
187. Chalapathi U., Bhaskar P.U., Sangaraju S., Al-Asbahi B.A., Park S.-H. $CuSbS_2$ thin films and solar cells produced from Cu/Sb/Cu stacks via sulfurization // Heliyon, 2024, V. 10, no. 6, pp. e27504. https://doi.org/10.1016/j.heliyon.2024.e27550
188. Zhang M., Wang C., Chen C., Tang J. Recent progress in the research on using $CuSbS_2$ and its derivative $CuPbSbS_3$ as absorbers in case of photovoltaic devices // Front. Optoelectron., 2021, V. 14, no. 4, pp. 450-458. doi: 10.1007/s12200-020-1024-0
189. Riha S.C., Koegel A.A., Emery J.D., Pellin M.J., Martinson A.B.F. Low-temperature atomic layer deposition of $CuSbS_2$ for thin-film photovoltaics // ACS Appl. Mater. Interfaces. 2017, V. 9, no. 5, pp. 4667-4673. https://doi.org/10.1021/acsami.6b13033
190. Chalapathi U., Poornaprakash B., Ahn C.H., Park S.-H. Two-stage processed $CuSbS_2$ thin films for photovoltaics: Effect of Cu/ Sb ratio // Ceram. Int., 2018, V. 44, no. 12, pp. 14844-9. https://doi.org/10.1016/j.ceramint.2018.05.117
191. Banu S., Ahn S.J., Ahn S.K., Yoon K., Cho A. Fabrication and characterization of cost-efficient $CuSbS_2$ thin film solar cells using hybrid inks // Sol. Energ. Mat. Sol. C., 2016, V. 151, pp. 14-23. doi: 10.1016/j.solmat.2016.02.013.
192. Raju N.P., Lahiri S., Thangavel R. Electronic and optical properties of $CuSbS_2$ monolayer as a direct band gap semiconductor for optoelectronics // *AIP Conf. Proc.*, 2021, V. 2352, pp. 020001. https://doi.org/10.1063/5.0052990
193. Nasonova D.I., Verchenko V.Yu., Tsirlin A.A., Shevelkov A.V. Low-temperature structure and thermoelectric properties of pristine synthetic tetrahedrite $Cu_{12}Sb_4S_{13}$ // Chem. Mater., 2016, V. 28, no. 18, pp. 6621-6627. doi: 10.1021/acs.chemmater.6b02720
194. Hathwar V.R., Nakamura A., Kasai H., Suekuni K., Tanaka H.I., Takabatake T., Ibersen B.B., Nishibori E. Low-Temperature Structural Phase Transitions in Thermoelectric Tetrahedrite, $Cu_{12}Sb_4S_{13}$, and Tennantite, $Cu_{12}As_4S_{13}$ // Cryst. Growth Des., 2019, V. 19, no. 7, pp. 3979-3988. https://doi.org/10.1021/acs.cgd.9b00385
195. Yaroslavzev A.A., Kuznetsov A.N., Dudka A.P., Mironov A.V., Buga S.G., Denisov V.V. Laves polyhedra in synthetic tennantite, $Cu_{12}As_4S_{13}$, and its lattice dynamics // J. Solid State Chem.,

2021, V. 297, pp. 122061. https://doi.org/10.1016/j.jssc.2021.122061

196. Tanishita T., Suekuni K., Nishiate H., Lee C.-H., Ohtaki M. A Strategy for Boosting Thermoelectric Performance of Famatinite Cu_3SbS_4 // Phys. Chem. Chem. Phys., 2020, V. 22, no. 4, pp. 2081-2086. doi:10.1039/c9cp06233e
197. Du B., Zhang R., Chen K., Mahajan A., Reece M.J. The impact of lone-pair electrons on the lattice thermal conductivity of the thermoelectric compound $CuSbS_2$ // J. Mater. Chem. A, 2017, V. 5, no. 7, pp. 3249-3259. https://doi.org/10.1039/C6TA10420G
198. Chetty R., Bali A., Mallik R.C. Tetrahedrites as thermoelectric materials: an overview // J. Mater. Chem. C, 2015, V. 3, no. 48, pp. 12364-12378. doi:10.1039/c5tc02537k
199. Suekuni K., Takabatake T. Research update: Cu–S based synthetic minerals as efficient thermoelectric materials at medium temperatures. // Appl. Mater., 2016, V.4, no.10, pp.104503-104513. doi: 10.1063/1.4955398
200. Levinsky P., Candolfi C., Dauscher A., Tobola J., Hejtmánek J., Lenoir B. Thermoelectric Properties of the Tetrahedrite–Tennantite Solid Solutions $Cu_{12}Sb_{4-x}As_xS_{13}$ and $Cu_{10}Co_2Sb_{4-y}As_yS_{13}$ ($0 \le x, y \le 4$) // Phys. Chem. Chem. Phys., 2019, V. 21, pp. 4547-4555. https://doi.org/10.1039/C9CP00213H
201. Powell A. V. Recent developments in Earth-abundant copper-sulfide thermoelectric materials. // J. Appl Phys., 2019, V.126, no.10, p.100901. doi:10.1063/1.5119345
202. Mikuła A., Mars K., Nieroda P., Rutkowski P. Copper Chalcogenide–Copper Tetrahedrite Composites—A New Concept for Stable Thermoelectric Materials Based on the Chalcogenide System // Materials, 2021, V. 14, no. 10, pp. 2635. doi:10.3390/ma14102635
203. Rikel' M., Harmelin M., Prince A. Arsenic-Copper-Sulfur System, In book: Ternary Alloys, Ed.: Petzow G., Effenberg G., Aldinger F., VGH, Weinheim, 1994, V. 11, pp. 109-127.
204. Kurz G., Blachnik R. New aspects of the system Cu-As-S // J. Less-Common Met., 1989, V. 155, pp. 1-8. https://doi.org/10.1016/0022-5088(89)90441-4
205. Prostakova V., Shishin D., Jak E. Thermodynamic optimization of the Cu–As–S system // CALPHAD, 2021, V. 72, p. 102247. https://doi.org/10.1016/j.calphad.2020.102247
206. Gasanova Z.T., Mashadieva L.F., Yusibov Y.A., Babanly M.B. Phase equilibria in the Cu_2S–Cu_3AsS_4–S system // Russ. J. Inorg. Chem., 2017, V. 62, no. 5, pp. 591-597. https://doi.org/10.1134/S0036023617050126
207. Gasanova Z.T., Aliev Z.S., Yusibov Y.A., Babanly M.B. Phase equilibria in the Cu-Cu_2S-As system // Russ. J. Inorg. Chem., 2012, V. 57, no. 8, pp. 1158-1162. http://dx.doi.org/10.1134/S0036023612050075
208. Babanly M.B., Gasanova Z.T., Mashadieva L.F., Zlomanov V.P., Yusibov Y.A. Thermodynamic study of the Cu-As-S system by EMF measurements with $Cu_4RbCl_3I_2$ as a solid electrolyte // Inorg. Mater., 2012, V. 48, no. 3, pp. 225-228. http://dx.doi.org/10.1134/S0020168512020021
209. Mashadiyeva L.F., Babanly D.M., Hasanova Z.T., Yusibov Yu.A., Babanly M.B. Phase Relations in the Cu-As-S System and Thermodynamic Properties of Copper-arsenic Sulfides // J.Phase Equilib. Diff., 2024. https://doi.org/10.1007/s11669-024-01115-w
210. Khvorostenko A.S., Kirilenko V.V., Popov B.I. Phase diagram of the As_2Se_3–Cu_2Se system // Inorg. mater, 1972, vol. 8, no. 1, p. 73-79..
211. Blachnik R., Kurz G. Compounds in the system Cu_2Se-As_2Se_3 // J. Solid State Chem., 1984, V. 55, pp. 218-224.

212. Mashadieva L.F., Gasanova Z.T., Yusibov Yu. A., Babanly M.B. Phase equilibria in the Cu–Cu_2Se–As system // Russ. J. Inorg. Chem., 2017, V. 62, no. 5, pp. 598-603. https://doi.org/10.1134/S0036023617050151
213. Mashadieva L.F., Gasanova Z.T., Yusibov Yu.A., Babanly M.B. Phase Equilibria in the Cu_2Se–Cu_3AsSe_4–Se System and Thermodynamic Properties of Cu_3AsSe_4 // Inorg. Mater., 2018, V. 54, no. 1, pp. 8-16. https://doi.org/10.1134/s0036023619060093
214. Hasanova Z.T. Thermodynamic study of the $CuAsSe_2$ compound by EMF method with solid electrolyte. // New Materials, Compounds and Applications, 2021, v.5, № 3, pp.205-211
215. Kopylov, N.I., Kaminsky, Yu.D. Novosibirsk: Sib.Univ. Publishing House, 2004, 367 p.
216. Muldagalieva R.A., Kuzgibekova K., Isabaev S.M. Heat capacity and thermodynamic functions of copper orthothioarsenate // *Russ. J.Phys. Chem*, 1996, V.70, pp.357-358
217. Skinner B.J., Luce F.D., Makovicky E. Studies of the sulfosalts of copper: III Phases and phase relations in the system Cu-Sb-S. // Economic Geology, 1972, V.67, pp.924-938. DOI:10.2113/GSECONGEO.67.7.924
218. Peccerillo E., Durose K. Copper–antimony and copper–bismuth chalcogenides—Research opportunities and review for solar photovoltaics. // MRS Energy & Sustainability, 2018, V.5, pp.1-56. doi: 10.15 57/mre.2018.10
219. Cui J., Zhang Y., Hao X., Liu X., Shen Y. Thermodynamic calculation of S−Sb system and Cu−S−Sb system. // Calphad, 2021, V.75, p.102362. https://doi.org/10.1016/j.calphad.2021.102362
220. Mashadiyeva L.F., Mammadli P.R., Babanly D.M., Ashirov G.M., Shevelkov A.V., Yusibov Y.A. Solid-phase equilibrium in the Cu-Sb-S ternary system and thermodynamic properties of ternary phases // JOM, 2021, V.73, no.5, p. 1522-1530. https://doi.org/10.1007/s11837-021-04624-y
221. Mashadiyeva L.F., Babanly D.M., Poladova A.N., Yusibov Y.A., Babanly M.B. Liquidus surface and phase relations in the Cu-Sb-S system, Chapter in book: Properties and Uses of Antimony, Ed.: David J. Jenkins, Nova Science Publishers, 2022, p 45-72. https://doi.org/10.52305/OJKB5395
222. Bryndzia L.T., Kleppa O. J. High-temperature reaction calorimetry of solid and liquid phases in part of the quasi-binary system Cu_2S-Sb_2S_3. // *American Mineralogist*, 1988, V.73, no.7-8, pp.707–713. https://doi.org/10.1016/0016-7037(88)90064-6
223. Tkachenko V.I., Regan M.Yu., Voroshilov Yu.V., Golovey M.I. / In the book: Abstracts of reports. IV All-Union. Council on chemistry and technology of chalcogens and chalcogenides. Karaganda: 1980. p.200
224. Babanly N.B., Yusibov Yu.A., Aliyev Z.S., Babanly M.B. Phase equilibria in the system Cu-Bi-Se and thermodynamic properties of selenobismuthides of copper. // Russ. J. Inorg. Chem., 2010, V.55, no.9, pp. 165-176. DOI: 10.1134/S0036023610090238

MİSİN MÜRƏKKƏB XALKOGENİDLƏRİNİN TERMODİNAMİK XASSƏLƏRİ

[1,2,3]M.B. Babanlı*, [1]L.F. Məşədiyeva, [1]S.Z. İmaməliyeva, [1]D.B. Tağıyev, [1,4]D.M. Babanlı, [5]Yu.A. Yusibov

[1]AR ETN akad. M. Nağıyev adına Kataliz və Qeyri-üzvi Kimya İnstitutu
[2]Bakı Dövlət Universiteti
[3]Azərbaycan Dövlət İqtisad Universiteti

[4]*Fransız - Azərbaycan Universiteti (UFAZ), Azərbaycan, Bakı*
[5]*Gəncə Dövlət Universiteti*
**e-mail: babanlymb@gmail.com*

Misin mürəkkəb xalkogenidləri maraqlı termoelektrik, fotoelektrik, optik, ion keçiriciliyi və digər xassələrə malik olan ən mühüm ekoloji təhlükəsiz funksional materiallar hesab edilirlər. Çoxsaylı tədqiqatların təhlili göstərir ki, bu birləşmələrin tətbiq xüsusiyyətlərinin yaxşılaşdırılması struktur və tərkibin manipulyasiyası ilə əlagəlidir. Belə proseslərin optimallaşdırılmasının effektiv həlli onların dərin termodinamik analizini tələb edir ki, bu da öz növbəsində müvafiq maddələrin fundamental termodinamik xassələri haqqında etibarlı məlumatların olmasını labüd edir. İcmalda misin bəzi p^1-p^3 elementləri ilə xalkogenidlərinin termodinamik xassələri üzrə tədqiqatların, o cümlədən müəlliflərin öz işlərinin nəticələri ümumiləşdirilmişdir. Ədəbiyyat analizi göstərdi ki, bu işlərin böyük əksəriyyəti elektrik hərəkət qüvvəsi (EHQ) metodunun müxtəlif modifikasiyalarından istifadə etməklə həyata keçirilib. Kimyəvi termodinamikanın bu tarazlıq üsulu ilə aparılan təcrübələrin planlaşdırılması və onların məlumatlarının emalı etibarlı faza tarazlığı mənzərəsi olmadan mümkün deyil. Bunu nəzərə alaraq, işdə termodinamik məlumatlarla yanaşı, EHQ üsulu ilə tədqiq olunan bir sıra sistemlərin bərk faza tarazlıqlarının diaqramları da təqdim edilmişdir.

Ədəbiyyat təhlili göstərdi ki, Cu-Tl-X, Cu-Ge(Sn)-X (X-S, Se, Te) və Cu-As(Sb, Bi)-S(Se) sistemlərində faza tarazlıqları və üçlü birləşmələrin termodinamik xassələri haqqında qarşılıqlı tənzimlənmiş məlumatlar mövcuddur. Cu-Tl-X və Cu-Sn-Se sistemlərin üçlü birləşmələrinin termodinamik funksiyaları EHQ metodunun iki modifikasiyası, yəni iki müxtəlif komponentin misin və ya talliumun (qalayın) parsial molyar funksiyalarının təyin etməklə müəyyən edilmişdiir. Misin qallium, indium və silisium ilə xalkogenidlərinin termodinamik xassələri praktiki olaraq öyrənilməmişdir, mövcud olan məlumatlar isə ziddiyyətlidir.

Açar sözlər: misin mürəkkəb xalkogenidləri, ekoloji təhlükəsiz materiallar, mis əsasında üçlü sistemlər, faza diaqramları, termodinamik xassələr, EHQ üsulu.

ТЕРМОДИНАМИЧЕСКИЕ СВОЙСТВА СЛОЖНЫХ ХАЛЬКОГЕНИДОВ МЕДИ

[1,2,3]М.Б. Бабанлы*, [1]Л.Ф. Машадиева, [1]С.З. Имамалиева, [1]Д.Б. Тагиев, [1,4]Д.М. Бабанлы, [5]Ю.А. Юсибов

[1]Институт катализа и неорганической химии им. акад. М. Нагиева МНО АР
[2]Бакинский государственный университет
[3]Азербайджанский Государственный Экономический Университет
[4]Французский – Азербайджанский университет (УФАЗ), Азербайджан, Баку
[5]Гянджинский государственный университет
*e-mail: *babanlymb@gmail.com*

Сложные халькогениды на основе меди относятся к важнейшим экологически безопасным функциональным материалам, имеющим большой потенциал применения, благодаря интересным термоэлектрическим, фотоэлектрическим, оптическим и др. свойствам, а также ионной проводимостью. Анализ данных многочисленных исследований показывает, что улучшение прикладных характеристик этих соединений связано с манипуляцией структуры и состава. Эффективное решение вопросов оптимизации таких процессов требует их глубокого термодинамического анализа, для которого необходимы надежные данные по фундаментальным термодинамическим характеристикам соответствующих веществ. В данном обзоре обобщены результаты работ, в том числе авторов, по термодинамическим свойствам халькогенидов меди с некоторыми p^1-p^3 элементами. Анализ показал, что подавляющее большинство этих работ выполнено

различными модификациями метода электродвижущих сил (ЭДС). Планирование экспериментов проводимых этим равновесным методом химической термодинамики и обработка их данных невозможна без наличия надежных по фазовым равновесиям. Учитывая это в работе помимо термодинамических данных приведены также диаграммы твердофазных равновесий ряда систем, изученных методом ЭДС.

Анализ показал, что для тройных систем Cu-Tl-X, Cu-Ge(Sn)-X (X-S, Se, Te) и Cu-As(Sb, Bi)-S(Se) имеются взаимосогласованные данные по фазовым равновесиям и термодинамическим функциям тройных соединений, причем для систем Cu-Tl-X и Cu-Sn-Se термодинамические функции тройных соединений определены двумя модификациями метода ЭДС путем определения парциальных молярных функций двух различных компонентов – меди и таллия(олова). В тоже время термодинамические свойства халькогенидов меди с галлием, индием и кремнием практически не изучены, а имеющиеся данные противоречивы.

Ключевые слова: сложные халькогениды меди, экологически безопасные материалы, тройные медьсодержащие системы, фазовые диаграммы, термодинамические свойства, метод ЭДС.